1999-01-01

Application of PVD Coatings to Enhance the Wear Life of Needles Used in the Textile Industry

Neil Donnelly
Technological University Dublin

Dublin Institute of Technology
Kevin Street
Dublin 8

Application of PVD coatings to enhance the wear life of needles used in the textile industry

Neil Donnelly
1999

Thesis submitted in fulfilment of examination requirements leading to the award of

Master of Philosophy

School of Physics

Supervisor: Dr. J.D. O'Mahony

I certify that this thesis which I now submit for examination for the award of Master of Philosophy, is entirely my own work and has not been taken from the work of others save and to the extent that such work has been cited and acknowledged within the text of my work.

This thesis was prepared according to the regulations for postgraduate studies by research of the Dublin Institute of Technology and has not been submitted in whole or in part for the award on any other Institute or University.

The Institute has permission to keep, to lend or to copy this thesis in part, on condition that any such use of the material of the thesis be duly acknowledged.

Signature Neil Donnelly **Date** 8/11/06

Acknowledgements

This body of work may, to some, be approximately 100 pages of typed script with a few nice pictures in it. To me, and hopefully to those who understand and can appreciate its content, it is much more than just a script. It is the summation of 20 months of work in a 'cutting edge' technology by myself and others who I would like to thank for their help and dedication to the project.

Firstly and above all others I would like to thank my industrial supervisor, Dr. D.P. Dowling (*Denis*). He gave me a great opportunity to do a piece of work in a very interesting field of study, and I thank him for it. I would also like to take this opportunity to thank my academic supervisor Dr. J.D. O'Mahony (*Des*) for his encouragement and for putting things in perspective for me at times when I needed it. Dr. Kevin Donnelly (or *Kev*), although not related, uttered the word "why?" more times than I care to remember. For helping me understand the true meaning of the word I will always be grateful. I would like to thank Dr. Miriam McConnell (*Mirr*) who suffered along with me during times of unquestionable frustration and who can fully appreciate the quotation "I have been to hell and back with magnetron sputtering". Her inexhaustible patience was an inspiration to me throughout the course of the work. Dr. Robert Flood and Dr. Gillian Lang have also helped me in some career decisions and for that I would like to thank them.

I would like to thank Mr. Kevin Armstrong and Ms. Clodagh Daly, my student companions for keeping me sane in a world full of tax-paying professionals, although now I must become one, Sorry!

Martin Fleming, whos initial training techniques, although questionable in some respects (atoms being compared to snooker balls?), gave me a great insight into the subject of plasma deposition. For that I am grateful. How could I possibly forget *The Doctor.*, as he so proudly calls himself. I would like to thank him for his extrasensory wit, but more importantly for his attention to detail in his explanation of such mechanics as turbine

power stations right through to glancing angle X-ray diffraction systems. I would also like to thank the Dr.s partner in crime, Peter Prior, for his X-ray fluorescence work and his humorous stories.

These acknowledgements could not possibly finish without the acknowledgement of "*the lads in metallurgy*" and their generosity in sharing their precious and highly expensive optical microscope with *a student*! Thanks for putting up with the slight myopia syndrome which I've been afflicted with.

I would like to thank Joe Keogh for at least sounding like he was genuinely interested in the project whilst others tried and failed. Also, thanks for the pulse generator, "It was old but it worked".

I would like to thank my parents for their continued support throughout the degree and for their financial assistance in obtaining my colourful but practical mode of transport.

And lastly, but not by any stretch of the imagination least, a special thanks goes to "*Aideen*" for her support and for sticking with a boring (*not old though*) physicist throughout the time it took to complete this arduous journey to a state of higher educational excellence.

To the aforementioned people I send a special thank you and to those who felt I should have said thanks but didn't then I also send you a special thank you!

A thank you must also go to the academic and industrial bodies of the Dublin Institute of Technology and Enterprise Ireland, respectively. Without their generosity and financial assistance this project could not have been brought its full potential.

This thesis is dedicated to

all who know me!

Table of contents

Abstract

Needles are used in the textile industry for weaving. In high volume textile production a problem is wear of the needle eyelet as the thread is pulled through. This wear results in a cost to the textile manufacturer both in needle replacement, but in many cases more importantly, lost production during needle substitution. The objective of this study was to examine the potential of wear resistant coatings deposited using the magnetron sputtering technique to increase the life-time of textile needles. Four coatings were evaluated, titanium nitride, titanium carbonitride, titanium diamond-like-carbon and a novel coating titanium nitride/molybdenum disulphide. These coatings were selected as they have already demonstrated enhanced performance in non-lubricated tooling applications such as for drills and reamers.

Initial deposition studies were carried out on flat steel substrates to facilitate the evaluation of the coatings. The deposition parameters varied were magnetron power, deposition pressure, and substrate bias during pretreatment and deposition. In order to reduce the number of experiments needed to determine the role of these various parameters on film quality the Taguchi experimental design technique was employed. The deposited coatings were evaluated using the knoop hardness, Rockwell indentation, scratch adhesion, scanning electron microscopy and a pin-on-disk wear tester. The latter technique measuring both film wear resistance and friction.

In order to replicate the movement of thread through the needle eyelet during textile production a test rig was designed and built. The rig consisted of a thread being drawn through the eye of the needle at high tension to cause wear. The damage to the needle eyelet was then evaluated by semi-quantitatively measuring the wear after a certain time period. It was found that there was a considerable reduction in eyelet wear in the case of the coated needle.

Chapter 1 : The deposition of thin films

1.1 Introduction

This thesis describes the application of wear resistant PVD coatings onto textile needles. The deposition and characterisation techniques used in the application of the coatings are also described. As there is a broad range of topics to be discussed, the thesis is divided into four main chapters.

Chapter 1 gives a background introduction into the area of coatings and the techniques by which they are deposited (See over). It describes how plasmas are used in the deposition of thin films, the thin film deposition system used in the project and the coatings that were deposited. The properties of the coatings investigated in the project are also discussed with an emphasis on how the deposition technique can affect these properties. These properties include adhesion, hardness, thickness, friction coefficient and wear resistance.

Chapter 2 concentrates on the techniques used in the characterisation of coatings including the scratch adhesion tester and Rockwell indentation test, microhardness tester, thickness tester and the pin-on-disk wear tester.

Chapter 3 will give an overview of the experimental setup used in the deposition of the coatings onto flat substrates. It will also introduce the Taguchi experimental design technique for parameter optimisation. An analysis of the properties of coatings deposited by the sputtering technique will be given.

Chapter 4 applies to the testing of the coated and uncoated needles using a wear tester which was designed and constructed as part of the project. This tester was used to simulate the wear that a needle would go through in a real life manufacturing process.

Using optical and profilometry techniques, the wear on each of the needles tested is analysed.

1.2 Plasma Technology

Perhaps the simplest definition of a plasma is an energetically excited ionised gas. The simplest example of a plasma is a lightening bolt. This occurs when a potential difference builds up between the clouds and the earth until the normally insulating air breaks down and an arc discharge forms. In the path of the arc, the gas (air) is energetically excited and contains many charged species such as positively ionised atoms and negatively charged electrons. The charged particles in a plasma such as this make them highly conductive and easily affected by magnetic fields. A considerable amount of energy must be given to a gas for it to become a plasma. Much of this high energy is often returned as heat. For this reason plasmas can reach temperatures of thousands of degrees Kelvin.

As a plasma cannot be described as a solid, liquid or a gas it is often called the fourth state of matter. Plasmas can be divided into two main categories. Thermal plasmas are high temperature plasmas that operate at atmospheric pressure and are generally used in applications such as welding. The other, and more important type in terms of this project, are called glow discharge plasmas. These plasmas are formed in a partial vacuum at pressures usually below 10^{-2} mbar. An inert gas resides between a cathode and an anode in vacuum. When an electric field is applied between the two electrodes electrons, which are naturally occurring in the gas due to radioactivity or cosmic rays, are accelerated away from the cathode at high velocity. Due to the high velocity, collisions occur in the gas causing excitation of electrons and ionisation of atoms. If an atom gains more energy by collision, its electrons can be promoted to higher energy levels for a short time. When the electron returns to its original energy level the excess energy is given out in the form of a photon, as shown in Figure 1.1.

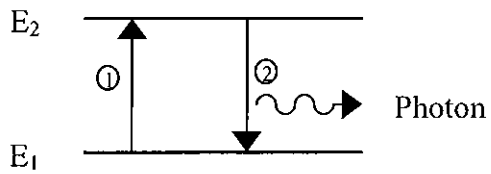

Figure 1.1:Energy release in the form of a photon of light due to the electronic decay from a higher energy band (E_2) to a lower one, typically the groundstate (E_2).

This process can be written as:

$$A + e^- \xrightarrow{①} A^* + e^- \xrightarrow{②} A + e^- + h\nu$$

where A is an inert gas, A* is its excited state, e^- is an electron, h is Plancks constant and ν is the frequency of the photon. It is these photons that give the plasma its characteristic glow. The quantity of electrons and the specific energy levels in the gas give the plasma its distinctive colour. For example, argon has a pink tinge when energised into a plasma form.

The majority of charges in a plasma are created by ionisation. This occurs when an electron moving at high velocity due to an electric field collides with an atom with sufficient force to knock an electron out of its energy level and leave the atom with an overall positive charge. This process is given by:

$$A + e^- \rightarrow A^+ + 2e^-$$

The electric field energy applied to ionise a gas can be delivered in different forms such as direct current (DC), radio frequency (RF) excitation and microwaves. The greater the electron density the greater the effectiveness of the process[1].

An interesting property of a plasma is that despite the charges being separated out, overall it is electrically neutral due to the electrons and ions being, to a good approximation, equal in density. It is hence termed quasi-neutral. If an electric field is created in the plasma the charged particles will act to reduce the electric field by redistributing

themselves. This response of the charged particles is called Debye shielding. For example, if two electrically charged surfaces are immersed in a plasma an electric field will be created. Species opposite in charge to that of the surface will be attracted to it thus shielding it from the plasma bulk. The plasma will therefore remain electrically neutral.

The use of plasma in industrial processing is becoming more common especially in the large scale production of integrated circuits and computer chips. Plasma is used in an etching process whereby the area of the chip not being etched is masked and the chip is electrically biased. Ions in the plasma etch the surface of the chip by striking it at high velocity. This creates vertical walls in the chip. This is called a plasma assisted technique and can allow increased production rates and high control and efficiency. Plasmas are also used in an ionitriding process for surface hardening. Using plasma, the surface properties of the material can be tailored to exact requirements.

In this project plasmas are used in the deposition of one material onto another forming a coating. This process is known as sputtering and is discussed in section 1.4.

1.3 Coating deposition techniques

In recent years plasmas have been used for many reasons from fluorescent lighting in buildings to etching in semiconductor fabrication. Another area in which plasma has become increasingly more popular in its use over the past twenty to thirty years is in the deposition of thin films onto substrates. There are many types of deposition systems. Some systems require the presence of a plasma whilst others rely on a chemical reaction for the deposition of a uniform coating. The majority of coating deposition systems can be separated into one of two main categories. Namely, chemical vapour deposition (CVD) and physical vapour deposition (PVD).

1.3.1 CVD

In 1969 a titanium carbide coating was developed on a cemented carbon tool. The coating had been deposited by a CVD[2] technique that had previously been developed in 1954[3]. This process was also used in the deposition of titanium nitride (TiN). The reaction took place in a hot wall reactor using mixtures of $TiCl_4$, N_2, H_2 and Ar. The reaction produced solid TiN and gaseous HCl:

$$TiCl_4 + 1/2\ N_2 + 2H_2 \rightarrow TiN\ (s) + 4HCl.$$

The H_2 was required in the reduction of the $TiCl_4$ and the Argon was used to enhance mixing. The solid TiN produced in the reaction settled on the substrate used producing a coating. These reactions took place at atmospheric pressure but could also occur at low pressure and at very high temperature (1023 K). The coatings were typically 5 to 10 μm thick. At that time little was known about the way in which the coatings altered the wear mechanism of the cutting tool but the extended lifetime of the tool was unmistakable. From then on new and varying techniques to enhance the wear lifetime of cutting tools was researched. Tungsten carbide and tool steel substrates were investigated and also multilayered coatings such as TiC/AlO_3. It was noticed that the high temperatures of reaction in the CVD process (Typically ~ 1000 °C) changed the properties of some substrates such as high speed steel and therefore limited the applications of the coatings. It was found that a physical vapour deposition (PVD) technique[4] used lower temperatures (Typically 350-500 °C) during its deposition and hence lowered its limitations as to the substrates that could be used.

1.3.2 PVD

The term PVD was originally intended to cover the deposition of single metals by the transport of vapour in a vacuum, without involving a chemical reaction. In recent years the term is more loosely used to describe any physical vapour deposition technique whether or not a chemical reaction takes place.

There are several types of PVD techniques including thermal evaporation, molecular beam epitaxy, thermal spray coatings and sputtering [5, 6]. Molecular beam epitaxy is typically used in the deposition of semiconductor coatings and therefore not relevant to this project. Thermal spray deposition is generally used to deposit thick films (> 10 μm) and also is not relevant to this project.

However, thermal evaporation and sputtering are similar in the sense that they are used to deposit the same type of coatings such as titanium carbide (TiC) and titanium aluminium nitride (TiAlN). The term 'thermal evaporation' is a general name given to processes such as electron beam evaporation[7], cathodic arc deposition[8] and laser ablation[9]. In these techniques either an electron beam, a flash arc or a laser, respectively, is used to vaporise material from the surface of a target creating a plume of ionised and neutral species which form a dense coating on the surface of a substrate. The sputtering technique was chosen as the deposition technique in this project and will be discussed in detail in the following sections.

1.4 The Sputtering technique

Sputtering is a commonly used technique in the deposition of thin films. Its popularity is due to the fact that it is very versatile and flexible in terms of the materials that can be sputtered. It is widely used in the semiconductor, hard disk drive, polymer extrusion, cutting, drilling, aerospace and automotive industries. In the biomaterial industry sensors are often manufactured using the sputtering technique and many of the films so deposited also have decorative and optical uses.

Sputtering is the process by which the surface of a solid material is ejected by a momentum exchange process, due to a high energy bombardment of the surface. A plasma is formed (See section 1.2) using a cathode made of the material to be sputtered,

called a target. The energetic particles, made up mostly of ions and neutral atoms, bombard the surface of the cathode forcing it to release material from its surface in an atomic form. Hence the material has been sputtered. In the sputtering process there is also the release of electrons and ions. Figure 1.2 illustrates the momentum exchange process.

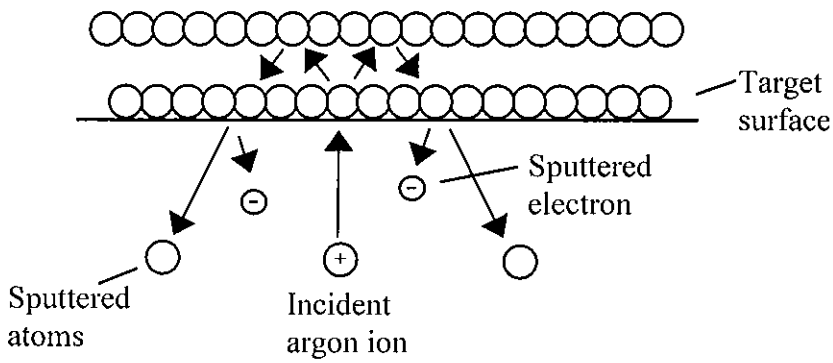

Figure 1.2: The sputtering of surface atoms with the release of high energy electrons due to the bombardment of the target surface by argon ions. The incident argon ion displaces surface atoms of the target which are "Sputtered" off. This "Sputtering" also produces electrons.

The sputtering yield is the number of atoms ejected from the target per incident ion. Depending on the relative molecular mass of the target material and the inert gas the sputtering yield can be increased or decreased[10]. The type of electric field applied to the target will also influence the sputtering. DC sputtering uses a DC electric field and is used to sputter conductive material from a target. Radio frequency (RF) sputtering has the advantage of being able to sputter from insulating targets. The entire process takes place inside a stainless steel chamber under a vacuum. Inside the chamber is the target, substrate and plasma. The schematic diagram in figure 1.3 illustrates the sputtering process.

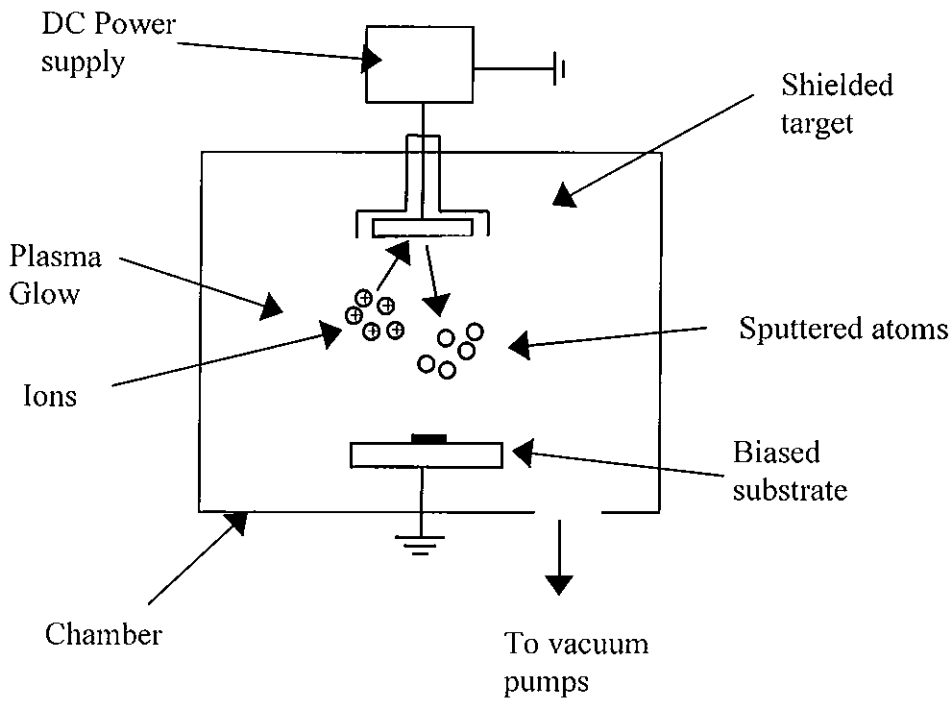

Figure 1.3: Schematic diagram of a DC glow discharge sputtering system. Note: The negative power supply (DC or RF) ignites the plasma, drawing the positive ions towards the target. The momentum exchange process occurs, releasing particles of the target material. The particles are intercepted by the substrate, forming a coating.

If, during sputtering, a surface is placed near to the cathode it will intercept atoms being released from the cathode and become coated with the cathodic material. This is known as 'sputter deposition'. If a reactive gas is introduced into the chamber while the sputtering process occurs then the species in the gas can react with the sputtered material forming a new coating. For example when sputtering aluminium, oxygen may be allowed into the chamber forming an aluminium oxide coating. This is called 'reactive sputter deposition'.

Often in a sputtering system the substrate to be coated will be biased. This occurs when a negative potential is applied to the substrate using a DC or RF power supply and ions are drawn towards the sample at high velocity[11]. This is mainly used in the pre-treatment stage before deposition occurs. This ion bombardment of the substrate gives two effects.

Firstly, cleaning it at an atomic level discarding contaminant material and secondly roughening the surface of the substrate. At the deposition stage biasing the substrate causes ions to bombard the surface while deposition is taking place. This has the effect of knocking the target atoms into place and hence giving a higher density coating.

As only a small percentage of the original energy of bombardment, incident on the surface of the cathode, takes part in the sputtering of particles from it to the substrate, then the majority of the energy is lost to target heating (which therefore requires the target to be cooled) and the remainder causes the emission of secondary electrons from the target. This inefficiency led to ways of maximising the efficiency of the incident energy.

Different types of sputtering techniques were designed such as Planar, Diode, Triode and Magnetron sputtering devices. The latter technique will be dealt with in detail in the following section.

1.4.1 Introduction to magnetron sputtering

During the sputtering process electrons which are involved in collisions in the plasma are projected outward from the target due to its negative charge. These electrons may become involved in collisions but also may recombine with ions or be lost to the walls of the chamber. To minimise electron losses and to increase the ionising effect of the electrons, magnetic fields are used in conjunction with electric fields. The use of magnetism in sputtering gave rise to the term magnetron. A magnetron consists of the target material with magnets fixed to its back in a certain geometry.

1.4.2 Magnetron sputtering

Magnetron sputtering incorporates the use of magnets into its design to control the efficiency and effectiveness of ion bombardment. The magnetic flux of the magnets can influence the electrons sputtered from the target but cannot control the larger sized atoms

or ions escaping from the target. By confining these electrons to a certain section of the target the efficiency will have improved dramatically and hence ionisation of the substrate also. Excess heating of the substrate is reduced due to secondary electrons being retained near to the surface of the target and also higher deposition rates can be achieved compared to other deposition techniques. The most widely used type is the planar magnetron, but there are also other geometrical arrangements that can be used such as the cylindrical, conical magnetron and the S gun magnetron [12 13].

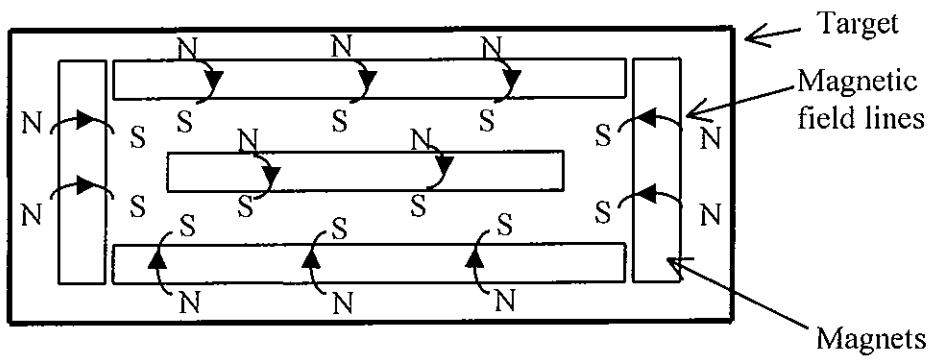

Figure 1.4: Diagram showing the geometry of the magnets placed on the back of the target. There are four outer magnets and a central one, the latter of which is weaker than the others producing an unbalanced effect.

Figure 1.4 shows the typical arrangement of the magnets on the back of a planar magnetron. The magnets used around the target are in fixed positions. Four strong magnets make up the outer rectangular magnet and one weaker magnet is fixed in the centre. This difference in strength of magnets means that the magnetron is "unbalanced". The fact that the magnetron is unbalanced increases the ionisation in a magnetic trap while decreasing the ionisation close to the target.

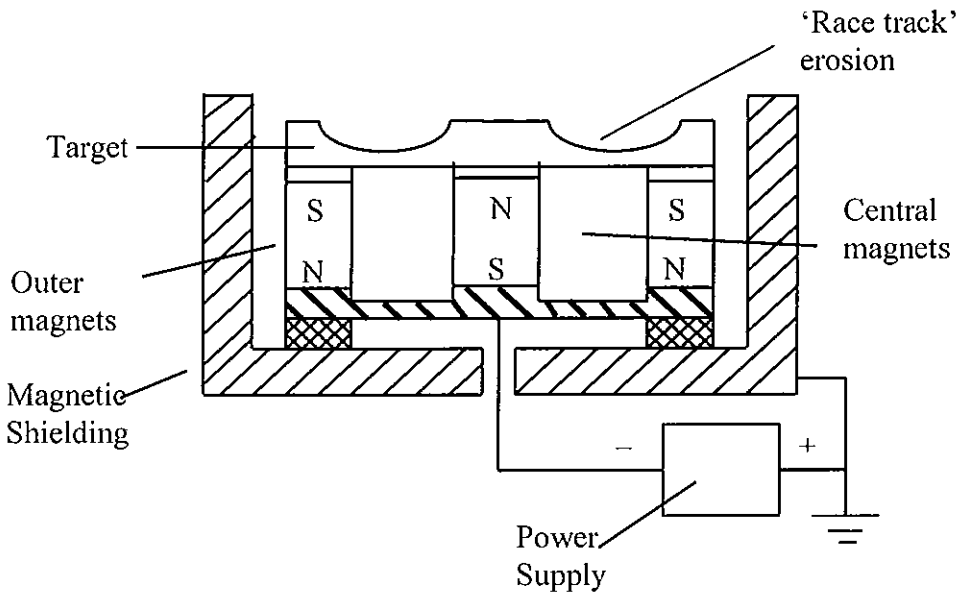

Figure 1.5: Cross section of a planar magnetron[14]. Note: the magnetron is isolated by the magnetic casing and the target is cooled by water which flows between and around the magnets and the back of the target.

The magnetron is encased in a metallic shielding which is grounded as illustrated in figure 1.5. The shielding is separated from the magnetron assembly by insulating caps. The power supply leads directly to the magnetic and target assembly. Each magnet is opposite in polarity to the magnet adjacent to it as illustrated in figure 1.4 and figure 1.5. The spaces in-between the magnets form a channel where water can flow in and out of the magnetron, continuously cooling the target. The water flows over the back of the target hence the name "directly cooled" magnetron.

1.4.3 Operation of the magnetron

In magnetron sputtering, magnets are geometrically positioned on the back of the target as illustrated in figure 1.4. The magnetic field coupled with the electric field therefore affects the particles that are sputtered from the target. Due to the geometry of the magnets, the magnetic field and electric field are parallel at one instance and perpendicular at another. The electric field is normal to the target so when the magnetic field is parallel to the electric field, the electrons are sputtered off the target and travel in a helical direction. The presence of the electric field accelerates the electrons and the

pitch of the helix lengthens. The radius of the helix can also vary. This prolongs the electron residence time in the plasma and thus enhances the probability of ionizing collisions. When the two fields become perpendicular to each other the electrons are bent back parallel to the target but still travel helically. This is illustrated in figure 1.6. As the magnets are orientated in a rectangle a "race track" shape is produced where the electrons hop around at high speed. This is where the majority of the ionisation occurs. The degree of ionisation occurring creates a type of "valley" in the shape of a rectangle or erosion track. The arrangement has been given the common name of "Race track".

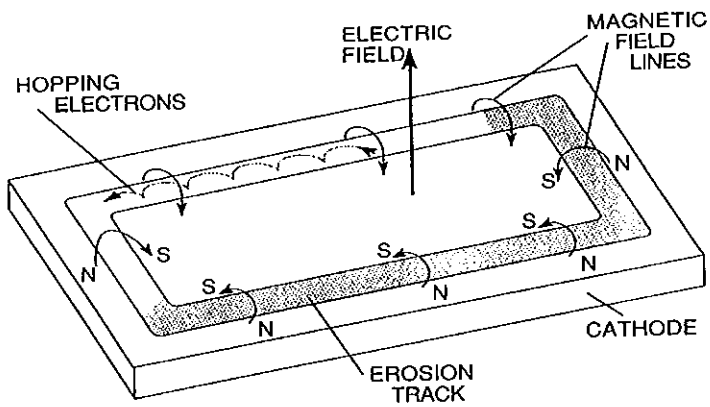

Figure 1.6: Schematic diagram, of a magnetron sputtering target, showing the electron as it travels in helical motion eroding the target. The target is eroded in a 'race track' shape. The magnets are on the underside of the target. It is the outer magnets which has the greatest influence on the degree of erosion, hence, the central magnet is not shown here.

1.4.4 Closed field system

The closed field system first described by D.G Teer[15] is based on the unbalanced magnetron technique developed by Window and Savvides[16]. The basis of the unbalanced system is that the outer magnets are made much stronger than the central one by either weakening the central or placing more permanent magnets on the outside. This still causes magnetic confinement of electrons close to the target, however, with the reduced magnetic confinement due to the weakened central magnet some of the secondary electrons can escape and enter a magnetic trap that has been made between the target and substrate as illustrated in figure 1.7. The electrons in the magnetic trap can cause further collisions with atoms in the plasma increasing the ionisation of the plasma.

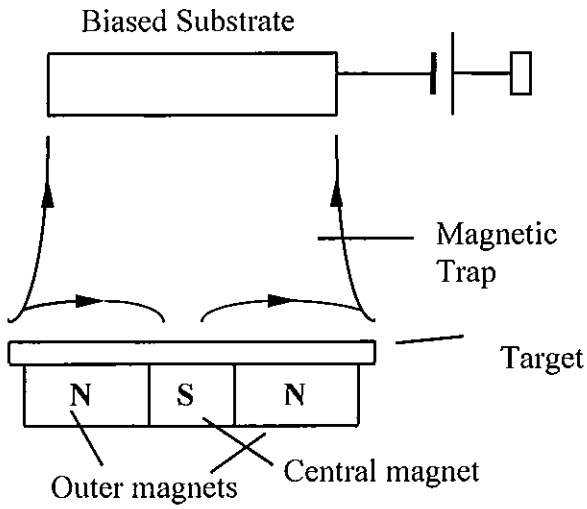

Figure 1.7: A diagram of a magnetron target creating a magnetic trap where electrons are enclosed. Note: the two outer magnets are strong while the inner magnet is weak. This allows for the magnetic trap.

The electrons follow the magnetic field lines where they bombard the substrate. Ions move in the same direction to preserve electrical neutrality and therefore produce ion bombardment of the substrate[17]. The bombardment of the substrate in this case is insignificant in comparison to the bombardment endured by the substrate during sample pre-treatment where a high negative bias occurs which attracts the ions to the sample at high velocity bombarding it. For this reason the coating being deposited is not sputtered off.

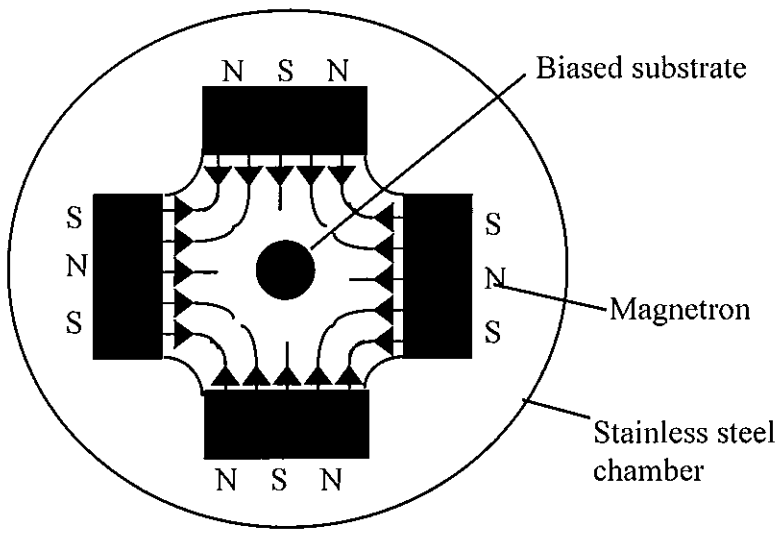

Figure 1.8: Diagram of a closed field system from an elevation above the chamber. The four magnetrons form the magnetic trap, which increases the ionisation density of the plasma.

Four unbalanced magnetrons are used to form the closed field arrangement, which operate simultaneously to create a localised magnetic trap around a central substrate holder. This is possible due to the adjacent magnetrons being of opposite polarity as illustrated in figure 1.8. Less electrons are therefore lost to the walls of the chamber. The closed field system has led to the increase in ionisation and a higher current density resulting in more uniform higher density coatings.

1.5 Coatings deposited

The primary use of any sputtering system and in particular the sputtering system described in section 1.4.2 is in the deposition of materials to form coatings. Thirty years ago there were very few coatings that were sputter deposited. Now there are many types of coatings ranging from hard low friction coatings such as chromium nitride (CrN) to soft extremely low friction coatings such as molybdenum disulphide (MoS_2). The coatings which are the subject of this project use titanium as the target material and are reactive sputtered with different gases including nitrogen and acetylene. Sections 1.5.1 to 1.5.4 describe the general properties of the coatings used in the project.

1.5.1 Titanium nitride (TiN)

TiN is deposited using a titanium metal target and nitrogen gas in an argon atmosphere. It is a very hard, low friction material that has been used in the cutting tool industry for approximately thirty years due to its excellent mechanical and tribological properties. It is also thermally stable, chemically inert, wear resistant, corrosion resistant and in recent years it has also become popular in areas such as the decorative industry, mainly due to its lustrous golden appearance.

The coating can also appear as a metallic silver or a brown colour, depending on the stoichiometry of the film. It is crystalline and has a high thermal and electrical conductivity making it useful in the production of diffusion barriers in integrated circuits. An important reason why industries have become so interested in the material is because it can be applied as a very thin layer to almost any shaped object by various deposition techniques.

Varying deposition techniques will give differing results. Many authors have published results for the mechanical (Hardness) and tribological (Friction) properties of TiN using different deposition techniques. Table 1.1 illustrates these differing results.

Deposition technique	**Hardness (Kg/mm^3)**	**Friction coefficient**	**Substrate**
Magnetron sputtering	3200	0.6-0.9	316 stainless steel
Electron beam	2100	0.63	35CD4steel
Reactive ion plating	2300	0.6	35CD4 steel
Cathodic arc	2836	0.547	JIS G4404 SKD61

Table 1.1: Lists the hardness, friction coefficient and substrate used for titanium nitride deposited coatings using various techniques. The hardness value is given in Vickers hardness (kg/mm^3) which is explained in section 2.4.

From table 1.1 it can be seen that the hardness and friction coefficient of TiN can vary substantially with the technique used to deposit the coating. These characteristics are also influenced by the substrate onto which the coatings are deposited which is illustrated in table 1.1.

Other influences are the reactive gas flow rate and the strength of the magnets on the targets which was investigated by Yeong Yan Guu *et al* [18] and I. Efeoglu *et al* [19], respectively.

The surface roughness of the coating can influence the characteristics of the film, the friction being the most influenced. If there are steep gradients on the surface, atoms will not adhere well to the material, but if the surface is perfectly smooth atoms again will adhere. For this reason it is important to clean the surface of the substrate at an atomic level. "This can increase interfacial solubility by creating high concentrations of point defects or stress gradients which enhance diffusion, resulting in the formation of pseudo-diffusion interfaces" [20].

1.5.2 Titanium carbonitride (TiCN)

Titanium carbonitride (TiCN) is a relatively new coating in comparison to TiN. TiCN has become popular in the drilling and cutting tool industry due to its increased hardness (Hv= 3000 Kg/mm^3 against Hv=2000 Kg/mm^3 for TiN) and lower friction coefficient due to the presence of carbon which acts as a lubricant. Examples of hardness values are given in table 1.2 . Note how the hardness of the coating is affected by the material used as a substrate. The difference between TiCN and TiN is that a carbon based gas, which in the case of these experiments was acetylene (C_2H_2), is added during deposition as well as the nitrogen to form the carbonitride. The coating is a sequence of layers deposited in the order of Ti - TiN -TiCN. Hence the term, multilayer coating.

In abrasive applications the higher hardness of TiCN and the presence of carbon to act as a lubricant makes it a superior coating to TiN in high speed applications[21]. TiCN also has a high thermal stability but its tribological properties can vary depending on the substrate and the stoichiometry of the film i.e. the content of carbon in the film[22]. The hardness of the film can also be affected by the microstructure (See section 2.7) and the carbon content. If the quantity of carbon in the coating is increased then the hardness will increase to a certain degree and the friction coefficient will usually decrease. There is no set stoichiometry for TiCN.

Deposition technique	**Hardness (Kg/mm^3)**	**Substrate**
Magnetron sputtering	3000	AISI 420
Cathodic arc	2800	35CD4 steel
Electron beam ion plating	2600	SKD61

Table 1.2: Lists the hardness values and substrate types for various deposition techniques.

1.5.3 Titanium diamond - like - carbon (Ti - DLC)

Ti - DLC is a relatively new coating (DLC being first deposited by Aisenberg and Chabot in 1971) in comparison to such coatings as TiN, although DLC itself has been used for many years. It has high hardness and extremely low friction. It is called diamond like carbon because its properties are similar to those of diamond i.e. high hardness and low friction. Its structure is mostly amorphous though whereas diamond is crystalline. It is used for machining aluminium, copper and stainless steel. It can also be used for punches, dies, engine components and for protecting machine parts. The titanium is sputtered and an excess quantity of acetylene is introduced into the chamber producing the carbon coating.

1.5.4 Titanium nitride/Molybdenum disulphide (TiN/MoS_2)

This is a new coating which combines the hardness and wear resistance of TiN with the low friction lubricating effect of molybdenum disulphide (MoS_2).

MoS_2 is the most widely used solid lubricant material for space applications[23] and also in sliding applications such as release mechanisms, pivoting hinges, telescoping devices and also rolling mechanisms such as precision bearings[24]. Current uses of MoS_2 are in the magnetic recording heads and disks because of its lubricity and diamagnetic properties. It is possible to use MoS_2 in these applications as it is chemically very stable and does not decompose to molybdenum and sulphur below 1100° C[11]. Also, it is resistant to most acids.

By depositing a very thin layer of MoS_2 (200 nm) onto a coating of TiN a wear resistant low friction coating can be deposited [25]. This type of coating is being investigated largely in the tooling and cutting industries.

1.6 Conclusion

This chapter has introduced the idea of depositing coatings onto substrates using techniques including the magnetron sputtering technique. It has also shown the types of coatings that can be deposited whilst concentrating on the four types concerned with this particular project.

1.7 References

[1] Cold Plamsa in Materials Fabrication: From fundamentals to Applications, A. Grill, IEEE Press, 1993.

[2] H. O. Pierson, Materials and Manufacturing, 8(4&5), 519-534 (1993).

[3] Helen E. Rebenne, Deepak G. Bhat, Surface and Coatings Technology, 63 (1994) 1-13.

[4] O. Knotek, F. Loffler and G. Kramer, Surface and Coatings Technology, 59 (19930 14-20.

[5] Handbook of thin film process technology, volume two, IOP publications Ltd, 1995.

[6] William D. Sproul, Surface and Coatings Technology, 81 (1996) 1-7.

[7] Electron beam evaporation, E. B. Garper, A1.2, Handbook of thin film process technology, IOP publications Ltd, 1995.

[8] Cathodic arc deposition, P. J. Martin, A1.4, Handbook of thin film process technology, IOP publications Ltd, 1995.

[9] Laser ablation, A. Morimoto and T, Shimizu, A1.5, Handbook of thin film process technology, IOP publications Ltd, 1995.

[10] J.C. Wang, M.T Hepworth and K. J. Reid, Plating and Surface Finishing, July 1990.

[11] Tribology-Friction and Wear of Engineering Materials, I.M Hutchings, Metallurgy and Materials Science, 1992, p. 26.

[12] The materials of thin films, Milton Ohring, Academic press, 1992, Chapter 3.

[13] Soon - Cheon Seo and Davis C. Ingram, Hugh Richardson, J. Vac. Sci. Technol. A 13(6), 1995.

[14] Magnetron Sputtering, A. S. Penfold, A3.2, Handbook of thin film process technology, IOP publications, 1995.

[15] D.G. Teer, Surface and Coatings Technology, 36 (1988) 901.

[16] B. Window and N. Savvides, j.vac. Sci. Technol., A4 (2) (1986) 565.

[17] R.D. Arnell, Surface and Coatings Technology, 59 (1993) 105-109.

[18] Yeong Yan Guu et al, Thin Solid Films, 302 (1997) 193-200.

[19] I. Efeoglu, Surface and Coatings technology, 57 (1993) 61-69.

[20] M. Ahern PhD thesis, Dublin City University (1991).

[21] J. Takadoum et al, Surface and Coatings Technology, 88 (1996) 232-238.

[22] Yeong Yan Guu et al, Thin Solid Films, 302, (1997) 193-200.

[23] M.R. Hilton and P.D. Feisschauer, Surface and Coatings Technology, 54/55 (1992) 435 - 441.

[24] Michael R. Hilton et al, Surface and Coatings Technology, 53(1992) 13 - 23.

[25] V.C. Fox, D.G. Teer, J. Hampshire, Teer Coatings Ltd, U.K, paper E1-2-9, Metallurgical Coatings and Thin films 1998.

Chapter 2: Coating Characterisation techniques

2.1 Introduction

High quality thin films possess a number of important properties which make each of them unique. Wear resistant films are noted for their chemical and erosive resistance, thermal resistance, electrical and thermal conductivity. These are properties of the material however. The properties which are important when assessing whether a high quality coating has been deposited or not are film-substrate adhesion, film thickness, film hardness and the friction coefficient of the film. Other important parameters when analysing the properties are the microstructure and morphology of the film and the stresses in the film. This chapter will focus on the examination of these properties and the techniques used to analyse the properties.

2.2 Adhesion

An important parameter in the determination of coating performance is its adhesion to the substrate. Adhesion is a macroscopic property that depends on the bonding across the interfacial region, the intrinsic stress, and the failure mode[1]. The bonding across the interface can be due to van der Waals forces, ionic, covalent or metallic bonds. The intrinsic stress is due to the nature of the coating. The failure mode will depend on the forces acting on the coating.

If the coating will not adhere to the substrate mechanical properties of the coating such as hardness and wear resistance become largely irrelevant. The process of adhesion can be broken into three parts:

(1) Fundamental adhesion
(2) Thermodynamic adhesion
(3) Practical adhesion.

In most situations it is an interphasial separation between film and substrate, not interfacial that denotes the adhesion (See glossary of terms). In these cases, the fundamental adhesion is the energy required to break the bonds at the weakest point in the interphase. The change in free energy when an interface is formed or separated indicates the thermodynamic adhesion. The practical adhesion is the force or work required to remove the coating from the substrate irrespective of the locus of failure i.e. whether failure occurred at the interface or somewhere in the interphase.

In this project it is the practical adhesion which is measured when analysing the coatings. Some of the factors which influence the practical adhesion of the coating are stresses in the film and mechanical properties of the film and substrate such as thickness, hardness and density. Due to the number of parameters influencing the adhesion there are over 300 techniques for analysing the adhesion of a film to a substrate[2]. The test most commonly used in the evaluation of hard wear resistant coatings on hard substrates, and the technique used in this work, is the scratch adhesion test which is described in detail in section 2.2.1.

2.2.1 Scratch adhesion tester

The generally accepted method of assessing the adhesion of hard coatings is the scratch adhesion test which, in its current form, was invented by Benjamin and Weaver[3]. This process involves deforming the coating-substrate interface by dragging a diamond stylus across the surface of the coating with an increasing load. However, it is difficult to express quantitatively the adherence because of the several parameters involved. There are intrinsic parameters such as scratching speed, loading rate, diamond tip radius and diamond wear. These are coupled with extrinsic parameters such as substrate hardness, coating thickness, surface roughness and friction coefficient. The mechanical resistance of the coating-substrate interface is characterised by a critical load (L_c) which is the minimum load at which damage by lack of adhesion can be observed.

2.2.2 Operation

The scratch adhesion tester used in this project is shown in figure 2.1. In this technique a diamond indenter is dragged across the coating with increasing load. At some load point the coating will flake off (Adhesive failure) or clip (chipping) (cohesive failure), this point is called the critical load L_c. The critical load has been described as 'the smallest load leading to unacceptable damage'. The scratch test does not directly measure the adhesion but rather the load required for disruption of the coating specimen, either at the interface or in the interfacial region. This load represents the practical adhesion[4]. Critical loads for ceramic coatings on hard steel substrates can typically lie anywhere in the region of 10-120 N depending on the testing instrument. A standard load of 5 N is applied to the diamond which lies on the coating thus initiating plastic deformation. The diamond is dragged along the surface at a constant increasing load causing full plastic deformation or fracture at very high loads. Therefore, a groove is left in the coating which can be analysed using optical microscopy as shown in figure 2.2.

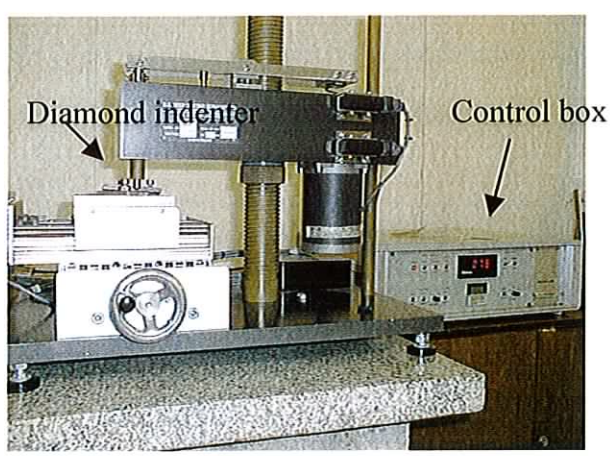

Figure 2.1: Photograph of a scratch adhesion tester. The diamond indenter lies directly above the motorised table, where the coating sample is placed. The speed of the table and loading rate of the diamond indenter are controlled by the control box.

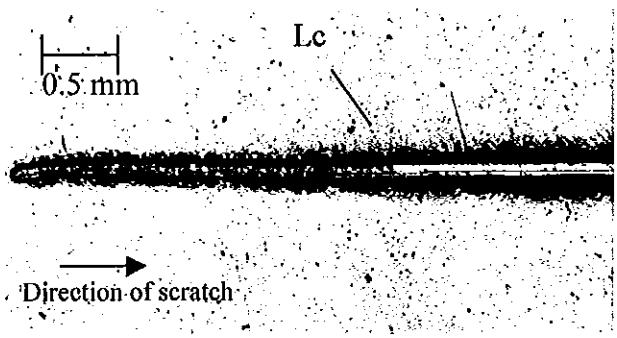

Figure 2.2: Photograph of a typical scratch on a Ti-DLC coating analysed by optical microscopy. The critical load (L_c) is the point at which the coating is removed.

Some of the features of the scratch are semi-ring cracks in the shape of the indenter. These are formed in front of the indenter due to stress and pass underneath it. This is illustrated in figure 2.2. 'kidney bean' shapes are formed on the side of the scratch and are due to a process known as "spalling". Spalling is the result of total delamination and corresponds to to an applied load greater than L_c [5]. This is illustrated in figure 2.3. In the case of brittle materials fragmentation or spalling of the coating occurs ahead of the indenter when the elastic energy is sufficient to result in detachment[1]. Microcracks also form alongside a scratch. This is a common occurrance and is indicative of a relatively normal amount of stress that a coating would be under. This is illustrated in figure 2.4

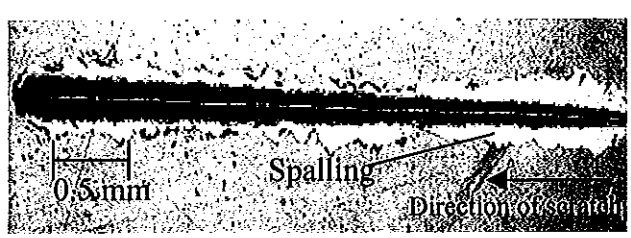

Figure 2.3: Typical scratch on an MoS_2 coating. 'Kidney bean' spalling or delamination on the sides of the coating has occurred owing to a load higher than that of the critical load. This has poor adhesive properties.

Figure 2.4: Photograph of a scratch on a DLC coating (mag=160), there are microcracks along the side of the scratch.

The scratch test is not an absolute method of adhesion failure but it is a comparative one that is an accurate indicator of adhesion when several samples are analysed together.

2.3 Rockwell indentation test

The Rockwell tester, shown in figure 2.5, evaluates both the adhesion between the coating and substrate and the cohesion in the coating. The test is carried out by deforming the coating using a hard cone shaped diamond indenter. A load of 100 kg or 150 kg is applied above the indenter which lies on the surface of the coating. The deformed surface can then be analysed using an optical microscope[6] and compared to a model of standard deformations as shown in figure 2.6. Each rating represents a different standard of coating cohesion and coating-substrate adhesion.

As illustrated in figure 2.6 the central circle in each of the six models is the imprint of the diamond indenter. In each case, there is a different quantity and geometry of cracking. HF1, as illustrated in Figure 2.6, has minor cracking around the indent indicating good adhesive and cohesive properties whilst HF6 has total delamination around the indent which represents poor adhesion and cohesion. In HF4 to HF6 the radial delamination has become progressively worse.

Figure 2.5: The Rockwell indentation tester. The diamond indenter lies above the sample holder. The load increases on the diamond creating an indent in the coating and substrate. The indent can be analysed for cracks.

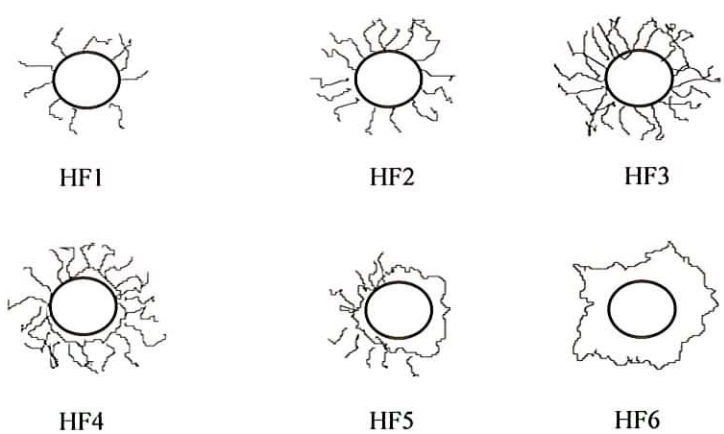

Figure 2.6: Schematic diagram of the six possible Rockwell indents on a coating-substrate system. HF1 represents minor cracking on the coating. Cracking becomes progressively more prominent until total delamination occurs, represented by HF6.

The Rockwell indent in figure 2.7 indicates cracking to some degree around the indent. The cohesive forces of the coating are weak whilst the coating remains adhered to the substrate

proving the adhesive forces to be strong. The coating in this case is given a Rockwell indentation rating of HF2 - HF3 as there is a high degree of cohesive cracking.

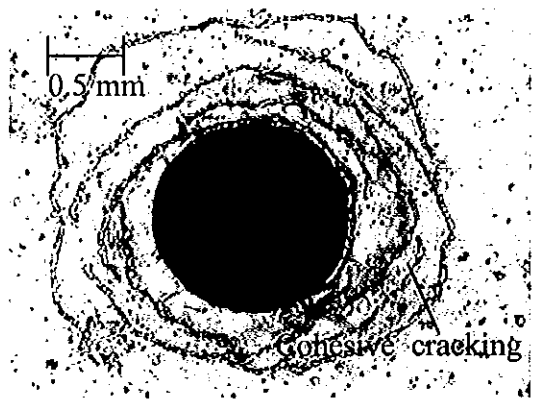

Figure 2.7: Photograph of a Rockwell indent on a Ti - DLC coating. The cohesive forces are weak whilst the adhesive forces are strong.

The photograph of the Rockwell indent in figure 2.8 illustrates the poor cohesive and adhesive forces of the coating-substrate interface. In this case delamination of the coating has taken place around the indent area. This coating is represented by HF6 of the model.

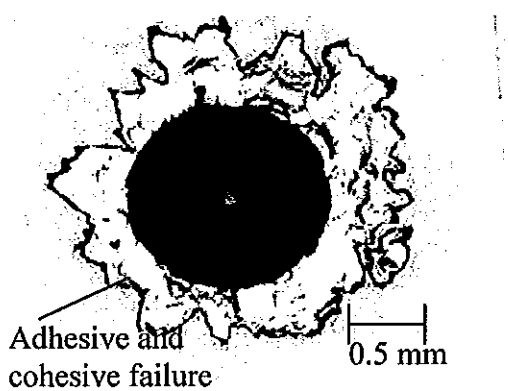

Figure 2.8: Photograph of a Rockwell indent on an MoS_2 coating. The total delamination of the coating around the indent indicates that there is poor adhesion and cohesion between the coating and the substrate.

2.4 Hardness

The hardness of a material has been defined as the ability of a material to withstand scratching (abrasion) or indentation by another body[7]. The hardness of a coating is influenced on a microscopic level by factors such as crystal structure, bond strength and density. On a macroscopic level the hardness is affected by such factors as coating thickness, coating-substrate interface and the indenter type and size. The hardness of a coating is of importance to this work as it has a large influence on the wear resistance of the coating along with the adhesion and friction coefficient. Measuring the hardness gives an indication of the wear resistance of the coating. There are several types of hardness measuring instruments but the one used in this work is the microhardness tester.

2.4.1 Microhardness tester

The hardness of a coating is determined by pressing an indenter into its surface and measuring the size of the impression. The hardness of the coating is inversely proportional to the size of the indent. The instrument used to measure the hardness is the microhardness tester. The term microhardness usually refers to indentation hardness tests where the load used is below 1000g and above 1g.

The microhardness tester, as shown in figure 2.9, operates by placing a known mass, usually 50 g, above a diamond tip which hangs directly above the coating to be tested. The weight will push the diamond tip into the coating causing an indentation. The size of the indentation can be related back to the hardness of the coating using a manual of standard indent sizes and hardness values. These tests can be performed by either of two types of intenters, Knoop or Vickers. The Vickers penetrates twice as far into the coating as the Knoop which could possibly cause the substrate to interfere with the results. Therefore, it is the Knoop indenter which is used in this work.

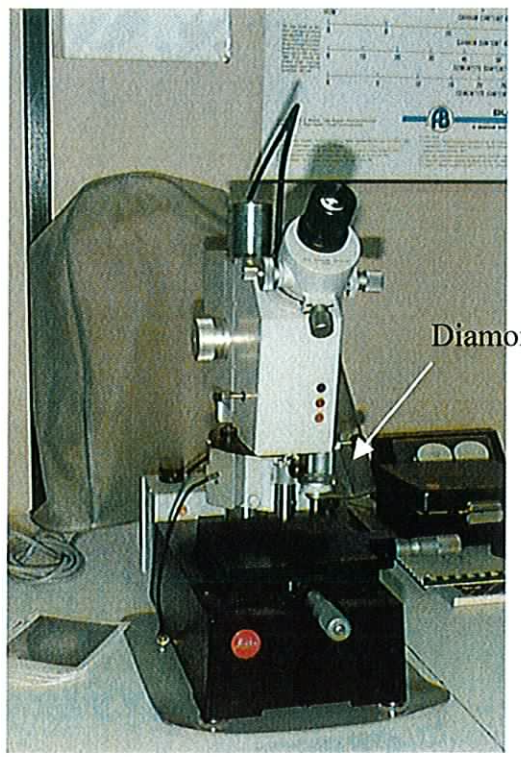

Figure 2.9: A photograph of a microhardness tester. The diamond lies above the sample to be tested. The load pushes the diamond into the surface of the coating indenting it. The size of the indent can be related to the hardness of the coating.

The Knoop indentation is performed with a diamond ground to pyramidal form that produces a diamond shape indentation having an approximate ratio between long and short diagonals of 7 to 1. The depth of indentation is about one thirtieth of its length. The two types of indenters are shown in figure 2.10.

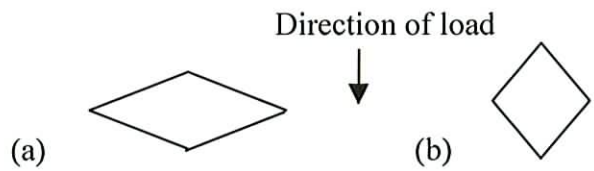

Figure 2.10: (a) Knoop and (b) Vickers indenters. The Knoop does not penetrate material to the degree that the Vickers indenter does and can therefore be used for coating analysis.

Each coating measured will have a particular knoop hardness number (Hk). Hardness values are measured in kg mm^{-2} but typically these units are not used and the value is given as X Hk where X is a number.

When using the microhardness tester the indenter should indent the coating no more than 10% of the thickness of the coating if accurate results are to be attained. Therefore low loads must be used leading to other problems such as a decrease in the size of the indent and therefore it is more difficult to measure optically. There is often a "trade off" between load and accuracy of result. It must therefore be stressed at this point that during the project it was found that some coatings were difficult to find a hardness value of due to deformation of the coating even at low loads. Also due to the limitations in the magnification of the microscope it was sometimes difficult to see the indentation in the coating.

2.5 Thickness

The thickness of the coating was measured by the Cap grinding method (more commonly known as the ball and crater method), described in European standard no. CEN/TC184WG5. This uses a steel ball with a low surface roughness and a motor and shaft to rotate the ball. This is shown in figure 2.12.

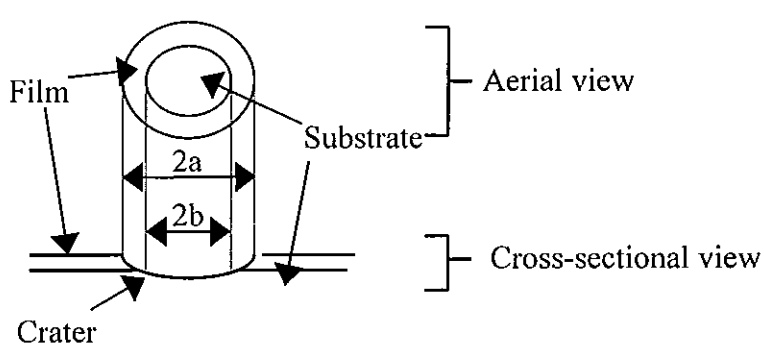

Figure 2.11: Aerial and cross-sectional view of the hemispherical area formed in the surface of a coating. The diameters of the circles are measured and the values can be substituted into a formula (Eqn. 1) to obtain the thickness of the coating.

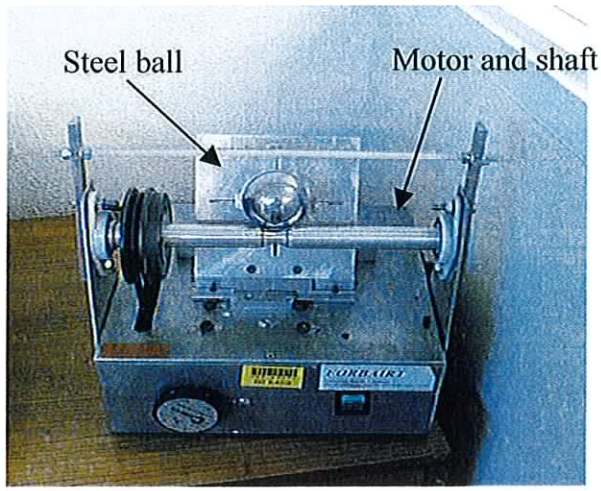

Figure 2.12: Photograph of the cap grinding thickness tester. The 5 cm steel ball rotates against the coating forming a crater. The thickness of the coating can be found by measuring the diameter of the apparent two circles in the crater.

Firstly the sample coating is locked in place. A very slight amount of 1/4 micron diamond paste is placed on the steel ball, which is 5 cm in diameter. The ball is supported on the motors' shaft and by the sample coating to one side. When the motor is switched on, the shaft turns the steel ball forcing it to wear away at the coating with the help of the diamond paste. A hemispherical section is worn into the sample. This contains what appears to be two circles, one inside the other. The diameter of each circle is measured using an optical microscope. The two circles and what they correspond to are shown in figure 2.11.

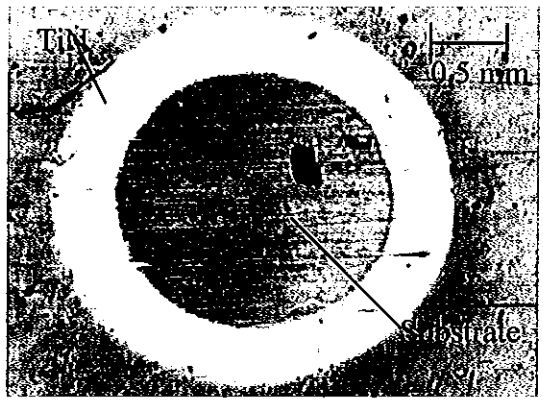

Figure 2.13: A photograph of a crater made in a TiN coating by a 5 cm steel ball. The two circles can be seen as can the substrate.

The radii of both circles can be substituted into a formula illustrated in equation 1.

$$t = \frac{1}{2R}(a^2 - b^2)^2$$

Equation 1: Equation to find the thickness of a coating where a and b are the radii of the outer and inner circle, respectively. R is the radius of the grinding steel ball. All dimensions are in microns.

2.6 Tribological properties

Tribology has been described as 'the science and technology of interacting surfaces in relative motion [8]. Tribology describes the action of friction and wear of surfaces in contact with one another. Friction is an important factor when characterising a wear resistant coating.

In a wear application the coating is moved against a counterface. On a microscopic level it would appear that the surface of both materials are covered in asperities as illustrated in figure 2.14. When the surfaces are moved against each other the asperities lock into one another and to move the surfaces further the asperities must bend or break. This action of bending or breaking causes both surfaces to have a high friction coefficient. Applying a coating to one of these surfaces has the effect of masking the asperities. The asperities on

the other surface have therefore nothing to "grip" onto and the system will have a low friction coefficient. If a coating deposited onto a surface has a low friction coefficient there should be less wear in the system. If the material has a low friction coefficient and is also hard, the wear on the system should be particularly low.

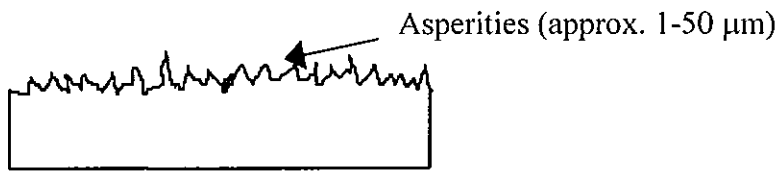

Figure 2.14: The surface of a material viewed on a microscopic level. The asperities are sharp peak like structures which form tight bonds when brought in contact with other asperities.

Wear resistance is the most important property with respect to this work. It is a property which encompasses many other properties. A coating with good adhesion, high hardness and low friction coefficient should have a high wear resistance. It is this wear resistance that can extend the lifetime of tools by up to 400%.

2.6.1 Tribometer (Pin-on-disk wear tester)

The friction coefficient and wear resistance of a coating can be measured using a pin-on-disk wear tester as shown in figure 2.15. This instrument consists of a pin or ball attached to a balanced arm. The balanced arm is attached to sensitive strain gauge. The sample is placed on a rotating disk and the pin lies on the sample. When the sample rotates changes in the friction coefficient between the pin and the surface of the sample are recorded by the strain gauge and the data is visually displayed on a PC. A load is usually placed on the balanced arm which increases the action of wear on the sample.

Figure 2.15: A photograph of a pin-on-disk wear tester. The balancing arm with the pin attached to it can be seen to rest on the sample to measure the friction coefficient of the coating.

Different coatings or materials will have different friction coefficients. Stainless steel, polished with 3 μm diamond paste steel has a friction coefficient of approximately 0.7-0.8. If a coating is deposited onto its surface the friction coefficient will generally decrease. TiN has a friction coefficient of approximately 0.5, on the addition of carbon to the coating the friction coefficient decreases to between 0.3 and 0.1 depending on the quantity of carbon in the film. MoS_2 has a friction coefficient of approximately 0.1 at atmosphere (~ 1000 mbar) but can decrease to 0.01 at pressures of 10^{-7} mbar[9].

2.7 Microstructure

When characterising a coating it is important to know whether the correct crystal structure has formed whilst in the deposition process. The crystal structure of a coating can be examined using a glancing angle X-ray diffractometer. This instrument can measure the crystal lattice orientation by reflecting X-rays off the surface of the coating and detecting the diffraction angle caused by the particular crystal lattice.

The grain structure that develops in a given deposition process is usually strongly influenced by what happens during film nucleation and subsequent growth[10]. This grain (Micro) structure gives an indication of how the coating will behave when used in an application. According to John A. Thornton the grain structure of a coating can be one of four types of structures or zones[11]. Three zones were first described by Movchan and Demshishin[12 13]. In 1973 this zone model was extended to magnetron sputtering where a fourth zone was added. These four zones are illustrated in figure 2.16. In this zone model the grain structure of a coating is classed into a different category or zone. These zones vary from columnar type structures to dense fibrous type structures. The microstructure zone diagram shows that there are two main parameters that influence the structure of the grain, argon pressure and substrate temperature. Argon pressure in this project is the argon flow rate. The pressure in the chamber can also be influenced by any other gas flow such as acetylene or nitrogen. The substrate temperature can be influenced by magnetron power and the level of substrate bias.

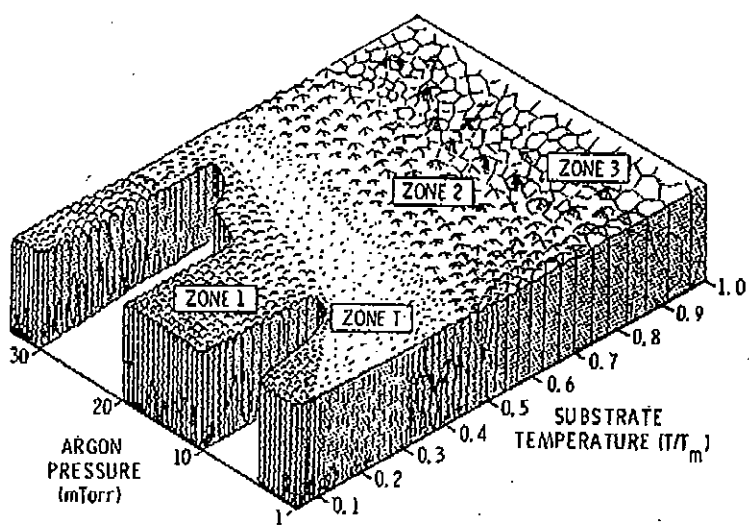

Figure 2.16: The microstructure zone diagram for thin films deposited by magnetron sputtering. Zone 3 consists of equiaxed grains with large columnar widths. Zone 2 has narrower columns. Zone 1 has more dense columns. Zone T is a transition state between zone 1 and zone 2. It consists of dense fibrous structure.

It has been shown that as both the argon pressure and substrate temperature change the structure of the coating also changes as illustrated in figure 2.16. At low substrate temperature the structure is generally columnar but column size broadens as argon pressure increases. This is a zone 1 type structure as illustrated in figure 2.17.

At higher substrate temperature the grains are still columnar but the grain boundaries have increased in width. This is called zone 2. By increasing substrate temperature again zone 3 type structures are formed consisting of equiaxed grains (See glossary of terms). There is another zone which has a dense fibrous structure and is found between zones 1 and 2 and hence is called the transition zone. The grain structure of a coating can be seen using a scanning electron microscope (SEM). This is the instrument used to illustrate the zone T type grain in figure 2.18. In this model it is the substrate temperature and argon pressure that affects the structure of the coating. Experimentally many other factors can influence the structure of the coating in the same way as the above factors. Some of the more important ones are magnetron power, substrate bias and reactive gas flow rate.

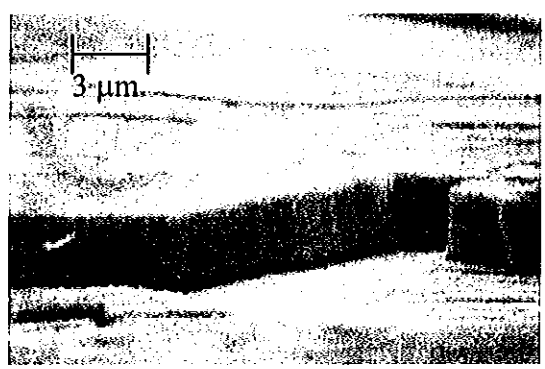

Figure 2.17: SEM micrograph of a TiCN coating illustrating zone 1 microstructure. The grain boundaries of the column can be seen.

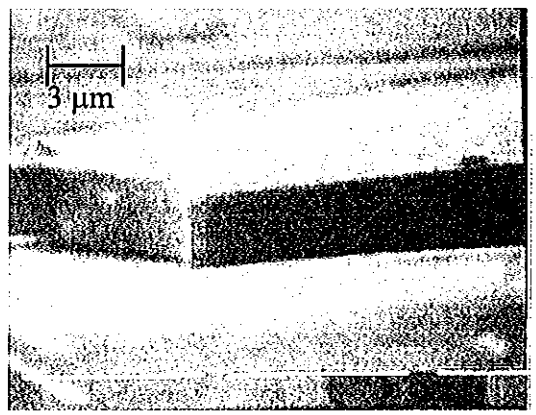

Figure 2.18: SEM micrograph of a MoS_2 coating illustrating a zone T type structure.

Thorntons model in this work is used as a classification model so that in later sections the structure of a coating can be referred to as a particular zone.

2.8 Multilayer Coatings

In recent years multilayer coatings have become increasingly more common. By combining the properties of different coatings the optimum coating can be created to suit certain applications[14]. The adhesion of the overall coating can also be improved by using multilayer components. An example of one such multilayer coating is Ti-DLC where coatings such as Ti, TiN, TiCN and Ti-DLC are deposited with increasing levels of wear resistance and decreasing levels of friction coefficients. It is a way of "Breaking the coating in". The base layer is deposited to ensure good coating-substrate adhesion. In these experiments the base layer is titanium and is usually 200-500 nm thick. Titanium is used as an underlayer for three reasons. Firstly, all layers can be deposited in the same chamber. Secondly titanium alleviates the difference in material properties between the substrate and the TiN, TiCN or Ti-DLC layers as it more ductile than the other coatings. Finally, the titanium underlayer reduces thermal stresses created during deposition or in the process of friction or wear[15]. Due to its higher ductility it can withstand more stress than TiN and will therefore not have

as high a fracture point. It allows extensive plastic deformation (See glossary of terms) at crack tips and deflects the crack into the plane of the coating due to its lower elastic modulus[16]. Ti/TiN coatings display an improved fracture resistance as compared to homogenous TiN[17]. The general sequence of coatings in a Titanium carbonitride multilayer coating is Ti/TiN/TiCN. In a multilayer coating of Ti-DLC the sequence is Ti/TiN/TiCN/Ti-DLC. Figure 2.19 is a diagram which represents the multilayer structure formed in the deposition of Ti-DLC.

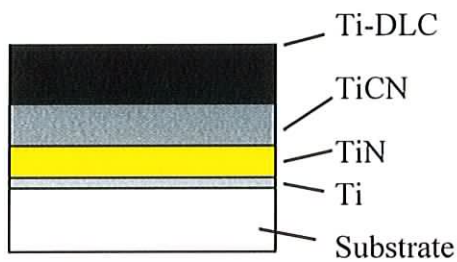

Figure 2.19: The Ti-DLC multilayer coating. The coating is made up of a multilayer of Ti, TiN, TiCN and Ti-DLC deposited one after another.

Columnar grain growth perpendicular to the substrate surface can be limited by a multilayer coating structure. These complex coating compositions favour fine grained structures and metastability with the possibility of amorphous states. Also there is an significant increase in the strength at the material interfaces, therefore thin hard multicomponent films possess greater strengths, elasticities and plasticities than those of a thicker coating[18].

2.9 Coating stresses

Like adhesion cohesion also plays a major role in the properties of the thin film whilst both of these properties are influenced by the types of stresses present in the thin film. It has been stated that virtually all metallic and compound films are in a state of stress[19]. The total stress in the film comprises of the intrinsic and extrinsic stress. The intrinsic stress or residual stress arises from the lattice structure of the coating itself. All the coatings featured in this work are in a state of high intrinsic stress. However their extrinsic stress can be influenced by parameters such as substrate bias and magnetron power. The increase or

decrease in these parameters can influence the density and hence the stress in the coatings. It is the high level of stress that will cause a coating to delaminate from the substrate and is therefore an important factor to consider when characterising a coating. The stress in the coating can be analysed but not measured by the Rockwell and scratch adhesion testers. The level of delamination of the coating when indented will give an estimation of the level of stress that the coating is under.

2.10 Conclusion

The properties illustrated in the previous nine sections are common to all coatings used in this project. The tests described are standard tests that are used to compare the properties of the coatings. It is essential that the results taken from these tests are used in a comparative capacity and are not used quantitativly. As there is such a wide scope of parameters involved in both the deposition and the properties of the coatings it would be difficult to find a test that would describe the parameters quantitatively.

2.11 References

[1] V.K. Sarin, Adhesion Measurement of Films and Coatings, K.L.Mittal (Ed.) VSP (1995), p.175-188.

[2] K. L. Mittal, Adhesion Measurement of Films and Coatings, VSP (1995), pp. 1-13.

[3] P. Benjamin and C. Weaver, Proc. R. Soc. London, Ser. A 254, 163 (1960).

[4] T. Z. Kattamis, Adhesion Measurement of Films and Coatings, VSP (1995), pp.143-160.

[5] J. Takadoum and H. Houmid Bennani, Surface and Coatings Technology, 96 (1997) 272-282.

[6] Nondestructive inspection and quality control, Metals Handbook, Vol. 11, 8th edition.

[7] Engineering materials, R.L. Timings., 5th impression, Vol.1, (1992).

[8] Tribology: Friction and wear of engineering materials, I.M.Hutchings, Edward Arnold, (1992).

[9] E. W. Roberts, Thin Solid Films, 181 (1989) 461-473.

[10] The material science of thin films, Milton Ohring, Academic Press, (1992), p. 41.

[11] John A. Thornton, J, Vac. Sci. Technol. A, Vol. N0. 6, Nov/Dec (1986).

[12] John A. Thornton, J. Vac. Sci. Technol. Vol. 11, N0. 4, July/Aug. (1974).

[13] B. a. Movchan and A. V. Demshishin, Fiz. Met. Metalloved. 28, 653 (1969).

[14] Coatings crank up tool performance, Ed Kubel (Ed.), Manufacturing Engineering, Jan. (1998).

[15] Yeong Yan Guu, JenFIn Lin, Chi-Fong Ai, Thin Solid Films, 287, (1996), 16-24.

[16] Michael Bromark, Mats Larsson, Per Hedenqvist, Sture Hogmark, Surface and Coatings Technology 90, (1997) 217-223.

[17] M.Y. He, F.E. Heredia, D.J. Wissuchek, M.C. Shaw and A. G. Evans, Acta Metall. Mater., 41, 4, (1993).

[18] O.Knotek, F. Loffer and G. Kramer, Surface and Coatings Technology, 59, (1993) 14-20.

[19] J. A. Thornton and D. W. Hofman, Thin solid films, 171, (1989), 5.

Chapter 3: Experimental setup and analysis

3.1 Introduction

Chapter 1 introduced the background to depositing coatings by the magnetron sputtering process. It has also dealt with the coatings that have been deposited by this technique and their properties. Chapter 2 has dealt with the characterisation techniques which were used in the analysis of coatings deposited onto flat stainless steel substrates and which will be discussed in section 3.4. General explanations for the equipment and coatings have been given in chapter 1. This chapter will explain specific equipment and techniques which are relevant to this project. The chapter will also introduce techniques such as experimental design and will give results of analysis performed on coatings that have been deposited by magnetron sputtering.

This project involved a two-tiered approach. Initially coatings were deposited onto flat stainless steel substrates so that the properties of the coatings could be easily evaluated using the characterisation techniques discussed in chapter 2. When optimised conditions for depositing coatings had been found on flat substrates then those coatings could be applied to industrial needles. Chapter 4 will concentrate on the application of the coatings to the industrial needles.

Chapter 3 will concentrate on coatings deposited onto flat samples. Due to the large number of parameters involved in the deposition of the coatings, a statistical computer package was used in the optimisation of these parameters. This will be described in detail in a later section in this chapter. The results of the properties of each of the coatings will be presented and discussed.

3.2 The sputtering system

In this project there were two sputtering systems used. The first was an old model magnetron sputtering system which used an RF biasing power supply manufactured by *Teer Coatings Ltd., England.*

The second system and more important system with respect to this project was a Teer Coatings U.D.P. 450 closed field unbalanced magnetron sputtering system (CFUBMS). The cylindrical stainless steel chamber housed two titanium targets (32 cm x 13.5 cm) in opposite configuration and which were 51 cm apart and had a rotating substrate holder centred between them. The sputtering gas used was argon and the reactive gases were nitrogen (zero grade) and acetylene (C_2H_2). Two MDX DC supplies powered the targets and an ENI DC supply (model no.- RPG - 50) gave a pulsed bias to the rotating sample holder.

If the pulsed supply is used to power a cathode (Target) in a sputtering process it is excellent at preventing target poisoning (See glossary of terms). When the RPG-50 is used as a substrate bias, as in this case, its prime use is in the cleaning of the substrate before deposition commences. During this process it can remove non-conductive material from conductive substrates such as steel tools and silicon wafers[1].

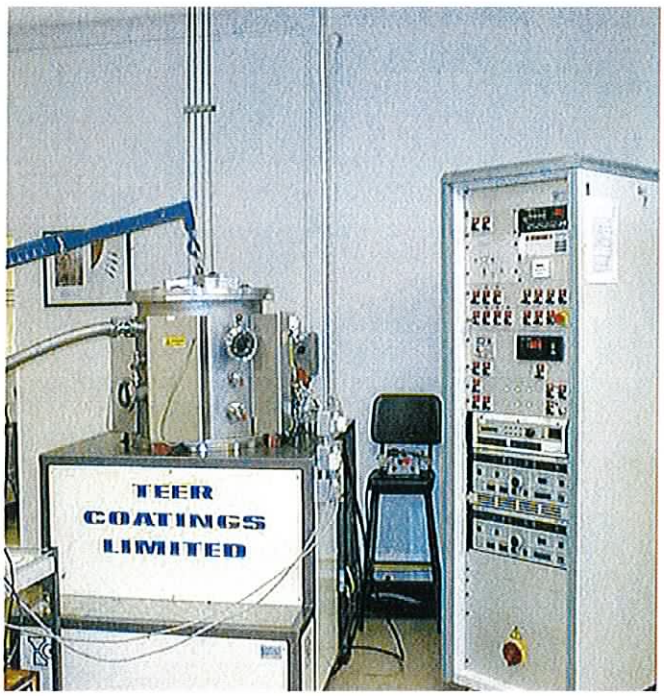

Figure 3.1: Closed field unbalanced magnetron sputtering system. On the right of the photograph is the rack cabinet which controls the DC power supplies, gas flow rates, optical emission monitor, pumping system, pressure gauges and valves. On the left of the photograph is the chamber which houses the four magnetrons and the pumping system below the chamber. There is also a hoist attached to the chamber lid. The portholes on the chamber can be used to view the plasma and substrate during deposition.

Due to problems encountered during the project with the U.D.P 450 CFUBMS system the older model magnetron sputtering system was used in the deposition of coatings onto the textile needles. This system was similar to the other except that it housed two magnetrons and had the facility to deposit from two targets instead of four. Also there was no closed field arrangement of the magnetrons. The bias was powered by an RF supply and the chamber had a different geometry to that of the other model. Therefore, there was a different set of deposition parameters used for this model. This system is shown in figure 3.2.

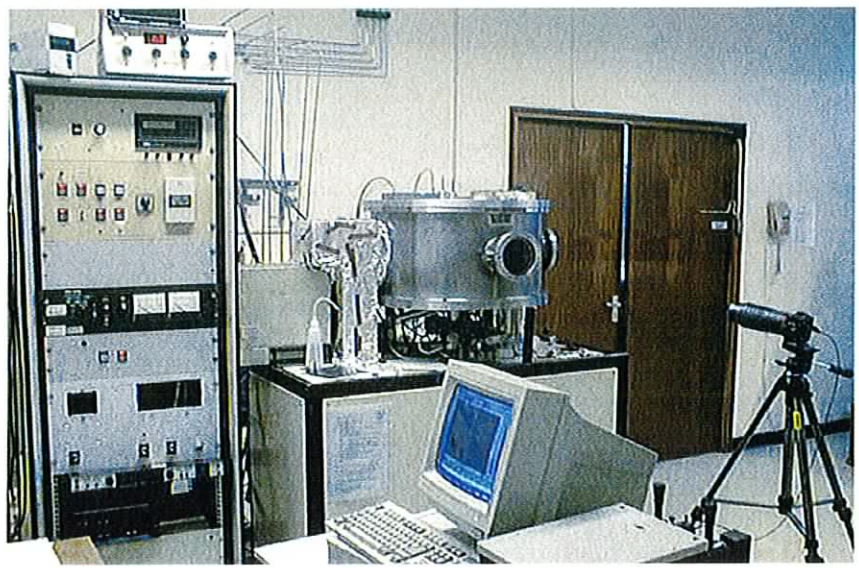

Figure 3.2: Magnetron sputtering system used in the deposition of coatings onto the textile needles. On the left is the control box, which controls the DC and RF power supplies, the pumping system, the gas flow rates, the pressure gauges and valves. On the right is the chamber which houses the two magnetrons and substrate holder. Below the chamber is the pumping system.

3.2.1 Vacuum pumping system

To generate plasma in a chamber requires a vacuum. In order to generate a magnetron plasma a vacuum of at least 10^{-3} mbar is required. For the magnetron system used in this project the pumpdown system consisted of a rotary pump and a diffusion pump which gave a base vacuum of ~10^{-6} mbar. The Edwards E2M40 was an oil-sealed, high vacuum rotary pump with gas-ballast capability and had an ultimate vacuum of 5 x 10^{-3} mbar with full gas ballast. During a typical deposition, the rotary pump would pump the chamber to 1.5 x 10^{-1} mbar in approximately 5 minutes whereupon the diffusion pump would take over pumping with rotary pump backing.

The diffusion pump was an Edwards Diffstak MK2 series 160/700. It had an ultimate pressure of 3 x 10^{-8} mbar but when pumping the deposition chamber a pressure not lower than 1 x 10^{-6} mbar was achieved after pumping overnight.

Any leaks in the chamber were detected using an IFICOM QUADREX PPC mass spectrometer connected via a port in the chamber. It was set at 40 a.m.u. to detect argon entering the chamber through the leak area. The argon entered the leak area by continuously letting argon gas flow over the outside of the chamber in areas where leaks were possible such as portholes and flanges.

3.2.2 Samples and their preparation

The samples used in these experiments were 2.5 cm in diameter x 0.5 cm thick stainless steel discs. They were polished using 3 μm diamond paste after being ground down using silicon carbide paper (120 grit/inch to 1200 grit/inch). The samples were washed in water and commercial grade acetone using an ultrasonic bath before being polished with the diamond paste. After being polished the sample was washed in high grade acetone and then in methanol. The sample was dried in air.

By extracting surface particles during handling and subsequent cleaning, it is possible to create microcavities during deposition. The higher the surface density of bonding sites on the substrate surface, the greater will be the number of nucleation sites for film growth. Therefore the preparation of the substrate surface prior to deposition will have a major influence on both the adhesion and the porosity of the films. For this reason the substrate is ion bombarded prior to deposition. This has two main functions. Firstly the surface is cleaned by bombarding contaminants remaining on the surface after solvent cleaning. Secondly the bombardment of the surface causes a surface roughening which increases the number of nucleation sites and hence allows for the deposition of dense films[2 3].

3.2.3 Deposition procedure

The deposition procedure is a standard method of coating deposition, the methodology of which has been determined over the course of many experimental depositions by the

surface engineering group, Enterprise Ireland. Any variation in deposition parameters (which will be seen in later sections) have been determined by the author.

The sample was placed in the chamber and the roughing valve switched on. The rotary pump pumped the chamber down to $1.5x10^{-1}$ mbar. At this point the high vacuum (HiVac) valve was switched which caused the diffusion pump to take over the pumping. The diffusion pump pumped the chamber down to the low 10^{-5} mbar range. This low pressure lowered the number of contaminants in the chamber which would interfere with the deposition of high quality films. The plasma was struck using the MDX power supplies and the magnetron current maintained at 0.2 A. The pulsed bias was set to -600 V for 30 minutes. This biasing of the substrate in this pre-treatment stage cleaned the target as described in section 1.4.

The first stage of depositing either the TiN, TiCN or Ti-DLC involved depositing a thin (200 nm) layer of titanium as described in section 3.2. The magnetron current was increased to 2.0 A and the bias was reduced to -180 V. Deposition took place for 5 minutes.

At this point nitrogen gas was introduced into the chamber reacting with the titanium metal and forming titanium nitride. The nitrogen level was maintained at 60 % using the optical emission monitor (OEM). The OEM consists of a spectrometer, readout device and a fibre optic cable held through a porthole in the chamber facing one of the targets. The spectrometer gave a read out of light intensity depending on the wavelength and intensity of the light. Once the titanium targets had been brought up to their maximum power level (2 Amps) the spectrometer gave an intensity readout. This readout was set to 100% (max. power) with no reactive gas present in the chamber The OEM uses the titanium emission intensity at a wavelength of 510 nm as a reference point of 100 %. When the reactive gas is introduced into the chamber the emission intensity of the titanium line decreases. The OEM can control this decrease to the nearest percentage using the spectrometer and piezoelectric valve connected to the reactive gas mass flow controller. In the case of TiN the OEM was set to 60 %. If TiN was the desired coating deposition took place for 60 mins to form a 3

μm film. If TiCN or Ti-DLC was the desired coating then the TiN was deposited for 15 minutes.

After 15 minutes of TiN deposition, the bias level was reduced to -45 V, acetylene gas was introduced into the chamber at a level of 60% and the level of nitrogen was adjusted to 2.3 sccm (Standard Cubic Centimeters per Minute). If TiCN was the desired coating then deposition took place for 45 minutes. If Ti-DLC was the desired coating then deposition took place for 20 minutes.

After 20 minutes of deposition the level of acetylene gas being allowed into the chamber was increased over a period of 10 minutes to give an OEM reading of 12%. At this point the Ti-DLC coating was deposited for 10 minutes.

3.3 Taguchi techniques

The deposition equipment and technique have been described in the previous section. However, depositing a high quality coating does involve each parameter being set and maintained at a particular point. For example during the deposition of TiN the substrate bias was set at -70 V. This setting along with all other settings were chosen using the Taguchi experimental design technique[4] described in section 3.3.1.

3.3.1 Introduction

As mentioned in section 3.2.3 there are a large number of parameters involved in the deposition of the coating. Therefore, a statistical experimental design software package was used to optimise the parameters. The important parameters involved in the deposition of high quality coatings are

- magnetron power (Sputtering current) during deposition and pre-treatment
- substrate bias level during deposition and pre-treatment
- chamber pressure

- sputtering gas flow rate
- reactive gas flow rate
- the use of interlayers
- target-substrate distance

All of the factors mentioned will affect the properties of the coatings in some way. It is the optimisation of these factors that will determine whether the coatings are high quality or not. The Taguchi statistical package was chosen as it is quick and user friendly.

3.3.2 The Taguchi technique

This experimental design program was developed by Genichi Taguchi to raise the calibre of quality engineering. It describes experimental procedure in terms of orthogonal arrays and linear graphs and uses them to design experiments based on a number of factors (parameters) and levels (setting of parameter). Depending on the orthogonal array used, different numbers of factors at different levels can be analysed. The common technique is to choose the factors which must be analysed. Each of the factors is assigned a level and a number of degrees of freedom. For example, if an experiment is affected by temperature and pressure then temperature and pressure are the factors. The factors can be set at different levels, for instance the temperature can be set at 100° C and pressure can be set at any level also. On each of the settings degrees of freedom can also be set such as 50° C and 150° C. The reproducibility of the experiment is important and for this reason care must be taken with respect to the sensitivity to 'noise'. In the case of this project 'noise' refers to the stability of the plasma during deposition, contamination on the substrate, inconsistency of gas flow and the qualitative characterisation of the coating. There are many other noise factors which also influence the experiments.

The convention for naming the arrays is given by $L_a (b^C)$ where:

a = number of experimental runs

b = number of levels of each factor

c = number of columns in the array

For example an L_9 (3^4) experiment means that there are four factors and three levels. Usually when describing the type of experiment the (3^4) convention is discarded and only the L_9 is used. On each factor there is a central level and two degrees of freedom giving the L_9 orthogonal array eight degrees of freedom. Another experiment is the L_8 (2^7) experiment. This has seven factors with two levels (2^7) each giving the experiment seven degrees of freedom. The most obvious choice when deciding on a particular Taguchi experiment is to choose the one which will give the most amount of information with the fewest number of runs. The L_9 and L_8 experiments are close in the number of runs that will need to be ran, 9 and 8, respectively. However, with only two levels it would take more experimental work to finely tune the parameters on the L_8 experiment. The L_9 has fewer factors but a higher range of levels. The choice of number of runs versus the number of factors amounts to what factors the experimentalist believes are the most influential on the outcome. Some factors can be taken out of the experiment for different reasons eg. A factor which cannot be controlled (atmospheric pressure or ambient temperature). There are also many other experiments which have a large number of factors and levels such as the L_{18} and the L_{27}.

3.3.3 Designing the experiments

There are several steps involved in designing the experiments. They are listed in order:

1. Define the problem
2. Determine the objective
3. Brainstorm -Group factors into control factors and noise factors
   -Determine levels and values for factors
4. Design the experiment - Select the appropriate orthogonal arrays for control factors
5. Conduct the experiment and collect the data
6. Analyse the data - Analysis of the data is carried out using the software package. The software allows the examiner to look at the average graphs and tables to find out which level in each factor had the most experimental influence
7. Interpret results - Select optimum levels of control factors

8. Run a confirmatory experiment to verify predicted results

3.3.4 Example: MoS_2 optimisation experiment

The Taguchi package is very useful when sputtering from a target whose optimised parameters have not been found previously. Due to the different relative molecular mass of each target material, parameters for deposition will also be different. In the case of this project the deposition parameters for molybdenum disulphide were not known. The following sections will give an example of how the Taguchi technique can be used to 'fine tune' the deposition parameters. It was decided that a Taguchi L_9 (3^4) orthogonal array experiment should be chosen as this takes into account four parameters and three levels of each.

The four parameters were

- Sputtering current
- Pre-treatment bias
- Deposition bias
- Argon flow rate

By using these factors and using a broad range of levels the optimisation field could be narrowed whereupon another experiment could be performed with a narrower range of levels. For example the levels chosen for the pre-treatment bias were -200 V, -300 V, -400 V. If the Taguchi program found that the optimum level should be -200 V then a new set of levels would be chosen close to this value such as -150 V, -200 V, -250 V. This could continue until accurate optimised parameters had been found. The parameters and levels are shown in table 3.1.

	Pre-treatment Bias/V	Deposition bias/V	Sputtering current/ Amps	Argon Level / Arb. Units
1	-200	-50	0.30	40
2	-300	-100	0.40	45
3	-400	-150	0.50	50

Table 3.1: The chosen factors, number of levels and their respective values. Each level has two degrees of freedom as described in section 3.3.2.

The experiments are listed in table 3.2.

	Pre-treatment Bias / V	Deposition bias / V	Sputtering current/ Amps	Argon level
(1)	-200	-50	0.3	40
(2)	-200	-100	0.4	45
(3)	-200	-150	0.5	50
(4)	-300	-50	0.4	50
(5)	-300	-100	0.5	40
(6)	-300	-150	0.3	45
(7)	-400	-50	0.5	45
(8)	-400	-100	0.3	50
(9)	-400	-150	0.4	40

Table 3.2: The factors, the number of experiments and their corresponding values are shown. As described in section 3.3.2 there are nine experiments. There are four factors (parameters) each of which has three levels.

Characterisation analysis was performed on the each of the nine experimental samples. They were reference coded mag 107 to mag 115. Characterisation was based on film thickness scratch adhesion, Rockwell indentation and microhardness. The results are tabulated in table 3.3.

	Thickness/μm	Scratch adhesion	Rockwell indentation	Micro-hardness	Comment
Mag 107	-	-	-	-	delamination
Mag 108	2.62	3	3	2	
Mag 109	3.83	4	4	4	
Mag 110	3.60	5	5	7	
Mag 111	3.20	2	2	6	
Mag 112	-	1	1	3	delamination
Mag 113	3.30	6	6	4	
Mag 114	1.50	7	7	1	
Mag 115	-	-	-	-	delamination

Table 3.3: The table illustrates the results obtained for thickness, adhesion (Rockwell and scratch) and the hardness for each of the nine coatings. Note, there are no results for those coatings which delaminated during or after deposition. The thickness of the films are given in microns whilst the other parameters are listed in order of arbitrary values of 1-7 where 1 represents a high quality coating and 7 represents a low quality coating.

Table 3.3 represents the optimised results for the Taguchi L_9 experiments. The scratch adhesion, Rockwell indentation and microhardness values were noted. These values were then convert to order of preference as this is the technique used by the Taguchi software. The numbers go in order of how one sample compared to another, number 1 being the coating with the desired properties and number 7 being the coatings with the least desirable properties Eg. in the case of microhardness, the coating with the highest hardness value got a no.1 rating and so on. Using the information in table 3.3, the software package will predict the optimum parameters for a coating of good adhesion or high hardness. It will also predict the parameters for a coating with high adhesion and high hardness. This is illustrated in table 3.4 where the Rockwell results represent the adhesion of the coating and the microhardness results represent the hardness of the coating.

	Pre-treatment bias/V	Deposition bias/V	Sputtering current/Amps	Argon level /a.u.
Rockwell	-400	-100	0.5	50
Rockwell and microhardness	-300	-50	0.5	50

Table 3.4: The optimised Taguchi results using the results from the Rockwell tests and the microhardness tests. The software package recommended these results based on the characterisation tests.

The result given in table 3.4 suggest that for high quality coatings with respect to microhardness lower biasing levels should be used during pre-treatment and deposition. The results do however suggest that the sputtering current should lie at 0.5 amps and that the argon flow rate should lie at 50 arbitrary units for high quality coatings. These results could now be used as the basis for a new set of experiments to be drawn up using the results as a focal point at which to base the levels around and therefore "fine tune" the values of the parameters.

The deposition parameters for TiN, TiCN and Ti-DLC coatings were all found in a similar fashion. Once the parameters were known the coatings were deposited onto flat stainless steel substrates and analysed using the techniques outlined in chapter 2.

3.3.5 Limitations of Taguchi

The Taguchi technique was used to find the parameters needed to deposit TiN, TiCN and Ti-DLC. There were certain limitations to the technique. As in the example in section 3.3.4 the parameters needed to deposit high quality coating were required. A broad field of parameters were chosen and using the Taguchi technique outlined in section 3.3.4 this field was narrowed. There is a limit to the degree that the field can be narrowed too due to the limitations of the instruments being used to control the parameters. For example the bias used in the deposition of the coatings was controlled by a power supply. However, due to

fluctuations in the chamber this voltage was difficult to keep at a steady state. Therefore as the field of parameters narrowed the margin of error associated with the bias increased. If the bias in one experiment was set at -200 V but it actually fluctuated by ±30 V and the bias in another of the Taguchi experiments was set at -300 V but actually fluctuated by ±30 V, then at any one point the error could be large in comparison to the intended value. This problem limited the accuracy of the Taguchi experiments when the field was narrowed significantly. In summation the Taguchi experimental technique can be used successfully when narrowing down broad ranging parameters but becomes less accurate as the parameters range becomes narrow.

3.4 Coating analysis

This section will concentrate on the results obtained for coatings deposited using the CFUBMS system. Using the Taguchi experimental technique optimised parameters have been found for all coatings in the next section. The results will describe the properties that have been found for the optimised coatings. These results will be compared to results reported elsewhere by other authors.

3.4.1 Titanium nitride (TiN)

Titanium nitride coatings were deposited onto flat stainless steel substrates by magnetron sputtering. The optimised coating was analysed. The coating was analysed by the characterisation techniques described in chapter 2. The initial analyse investigated the microstructure and morphology of the coating.

The structure of TiN was found to be face centred cubic crystalline lattice with an orientation mixture of (111) and (220) and (311). This is similar type structure to that of NaCl. This type of structure allows a high mobility of electrons which in turn contributes to the materials overall high electrical and thermal conductivity[5]. The crystal lattice orientation is illustrated in figure 3.3.

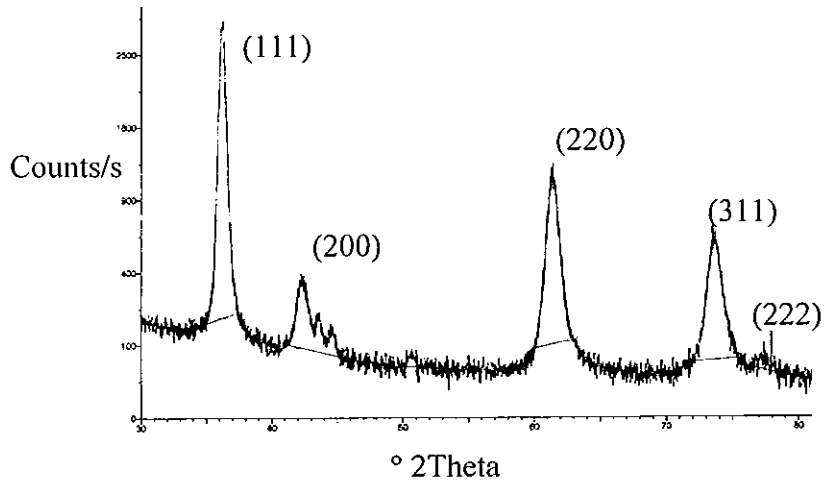

Figure 3.3: Glancing angle XRD pattern for TiN illustrates that this coating has a (111) orientation but also has strong crystal phases such as (220) and (311).

It has also been found that at concentrations of over and under stoichiometry TiN has a preferred orientation of (200) or (220). The substrate used to deposit the coating onto also affects the film texture[6].

Using Thorntons' classification model described in section 2.7 the optimised TiN coating was found to have a structure in-between that of zone T and zone 1. It has a definite columnar structure[7 8 9] but its grain boundaries are not clearly defined giving a more dense type structure. This columnar structure is illustrated in figure 3.4.

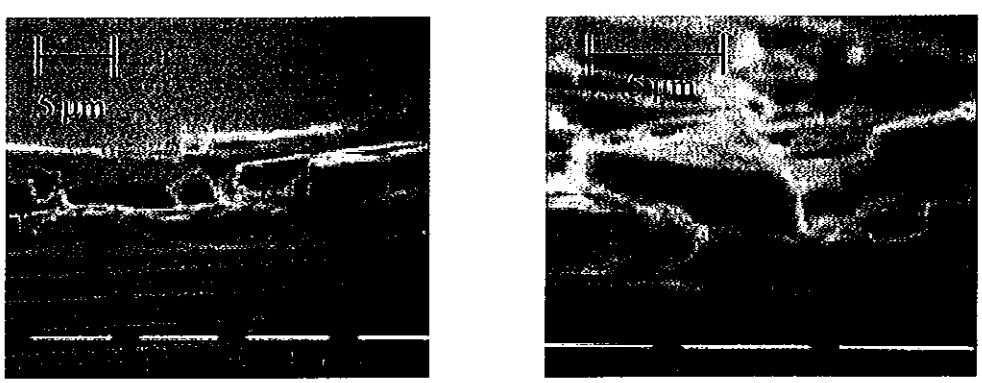

Figure 3.4: Micrographs of the structure of TiN showing that TiN has a dense columnar type structure with a Thornton classification of zone T or zone 1.

The dense structure is usually indicative of a high bias voltage during deposition of the coating[10 11]. The high bias has the effect of knocking the atoms into place and increases densification.

The adhesion of the TiN to the stainless steel flat sample was investigated using the scratch adhesion tester described in section 2.2. The adhesion of two different thickness' of TiN were investigated, 1.5 μm and 2.5 μm[12]. The thicker of the two had a critical load of 20.5 N whilst the other had a critical load of 21 N. Both of these results are adequate for good adhesion. Adhesion results have been reported with critical loads ranging from 5 N up to 160 N [7 13-14]. Adhesion can be affected by almost any parameter. It has been reported that a higher hardness TiN coating will usually have a lower adhesion. Also highly polished surfaces have a greater adhesion than those with a rough surface, hence the reason why all substrates are polished to 3 μm.

It has been reported that the adhesion of the coatings is affected by the thickness as it is raised from 1 μm to 5 μm[13]. In these experiments the thickness was not changed significantly enough to see a notable change in adhesion.

The adhesion and the cohesion of the coatings was shown using the Rockwell indentation test described in section 2.3. The two coatings gave a HF value of 1. An image of the 2.5 μm coating is shown in figure 3.5. This HF value was another indication that the film-substrate adhesion was excellent.

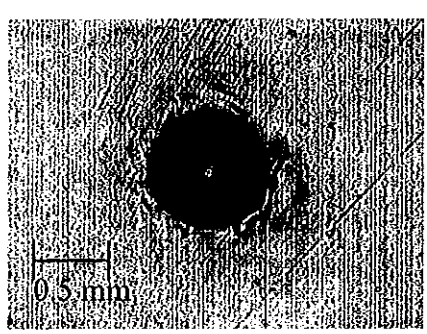

Figure 3.5: Photograph of a rockwell indentation for TiN-2.5 μm (HF1).

The knoop hardness of the TiN coatings was found to be between 1700 and 1800 mm kg^{-2}. These figures are consistent with other authors. Ward et al found the hardness of TiN deposited by magnetron sputtering to be 2188 mm kg^{-2} using the Vickers hardness measuring technique with a 50 g load. Y.Y. Guu found the hardness of TiN deposited by cathodic arc ion plating to be 1432 mm kg^{-2} again using the Vickers hardness measuring technique. The hardness values given can vary depending on parameters such as coating thickness, deposition technique, load used and indenter type. A hardness value in the region of 2000 mm kg^{-2} is regarded as satisfactory for TiN coatings.

The friction coefficient of optimised TiN has been found to lie in the 0.5-0.6 region as illustrated in figure 3.6.

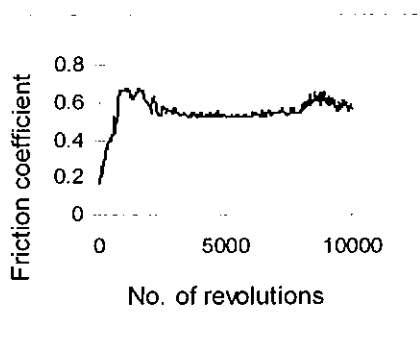

Figure 3.6: Friction coefficient of a TiN coating. Its friction coefficient range lies between 0.5 and 0.6.

The friction coefficient of TiN is lower than other materials such as stainless steel due to a TiO_2 layer which is formed as the TiN coating rubs against its counterpart which in the case of figure 3.6 is a tungsten carbide ball. The TiO_2 layer forms a lubricant between the coating and its counterpart which lowers the friction between the two bodies.

3.4.2 Titanium carbonitride (TiCN)

Titanium carbonitride (TiCN) was deposited onto flat stainless steel substrates and analysed by the characterisation techniques outlined in chapter 2.

TiCN has a face centred cubic crystalline structure similar to that of TiN. It has a (111) preferred orientation as illustrated in figure 3.7. It also exhibits weak (200) and (220) peaks. The relative strength of these peaks can be increased by an increase in the quantity of carbon in the film[14].

TiCN has been found to posses columnar type crystalline grains. Its structure lies between zone 1 and zone T by the Thornton classification model. Its structure is illustrated in figure 3.8 and its grain boundaries can be clearly seen.

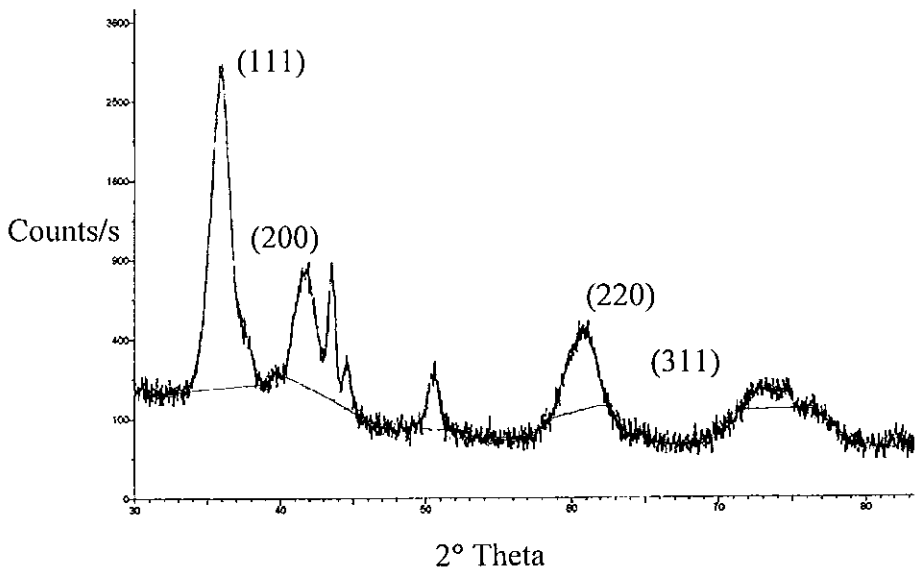

Figure 3.7: XRD diffraction pattern for TiCN. The coating exhibits a preferred orientation of (111) and weak (200) and (220) peaks.

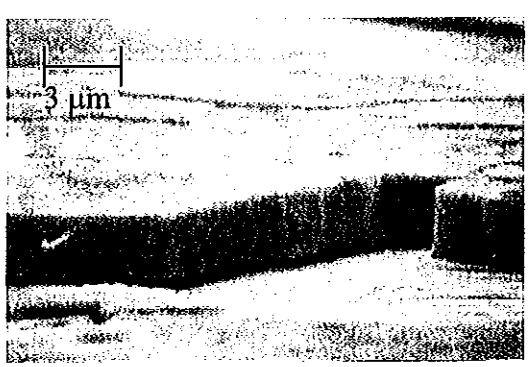

Figure 3.8: A photograph of a fractured coating TiCN which illustrates its dense columnar structure.

The adhesion of a 1.5 μm and 2.5 μm thick coating of TiCN was investigated using a scratch adhesion tester. The adhesion of the thicker coating was found to be 24 N whilst the other was found to be 19 N. Both of these results are adequate for use in tool coating applications.

A Rockwell test was performed on the two coatings. The thicker of the two gave a HF value of 1 indicating excellent film-substrate adhesion and also film cohesion. The 1.5 μm film gave a HF value of 2 which follows the trend of the scratch adhesion results.

The hardness of the two coatings was measured with a microhardness tester. The results of the hardness tests on the 1.5 μm and 2.5 μm coatings were 1730 and 2105, respectively. The indentation on the thinner of the two coatings was influenced by the substrate which resulted in giving a similar value to the 1.5 μm TiN coating in the previous section. The result for the 2.5 μm coating are in accordance with other authors[15,16]. These authors have shown that the higher the content of carbon in the coating the higher the hardness value. In this project this hypothesis was also shown. A coating was deposited with an excess quantity of carbon, in the form of C_2H_2, in the chamber. This coating had a hardness value of over 4000 Hk. The adhesion tester gave a value of 6 N as its critical load and the Rockwell indentation tester gave a HF value of 4. These adhesion results are illustrated in figure 3.9.

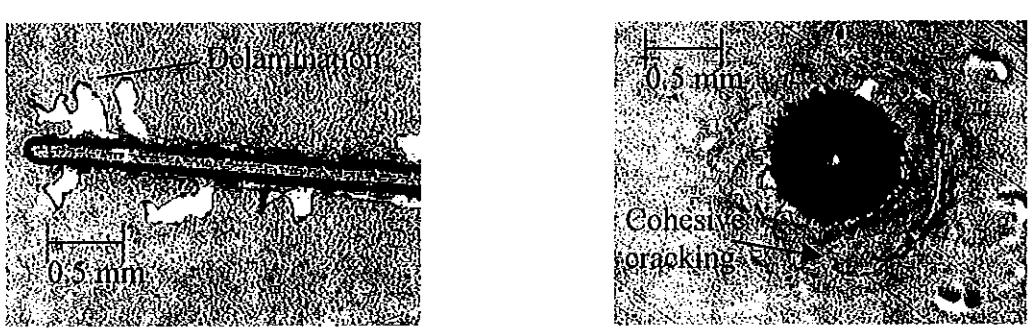

Figure 3.9: Photographs of (a) a scratch (b) a Rockwell indentation on a TiCN coating with excess carbon. The scratch illustrates the poor adhesive forces between the coating and substrate and the Rockwell indentation illustrates the poor cohesive forces in the coating.

The friction coefficient of TiCN of thickness 1.5 μm and 2.5 μm are shown in figure 3.10.

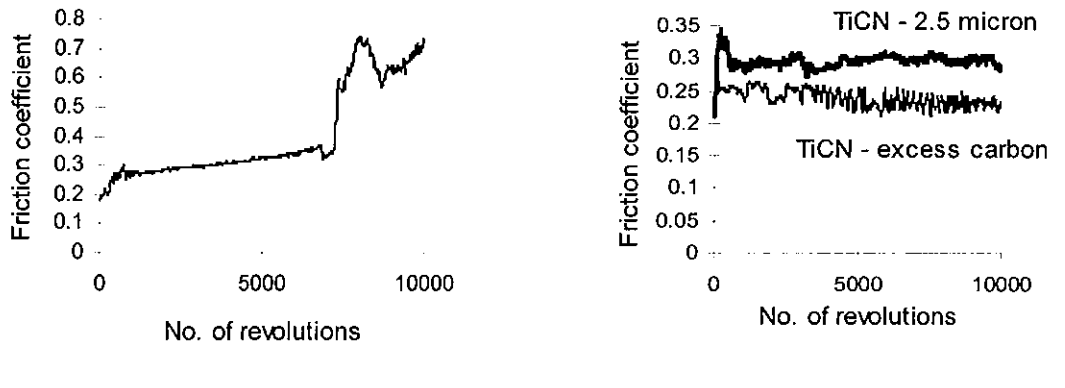

(a) (b)

Figure 3.10: Graphs showing the friction coefficient of (a) TiCN 1.5 μm thick and (b) TiCN 2.5 μm thick and TiCN with excess carbon.

TiCN in both the 1.5 μm and 2.5 μm thickness cases have a friction coefficient of approximately 0.3. In figure 3.10 (a) the pin on the pin-on-disk tester wore through to the substrate at approximately 7000 revolutions. The thicker coating has increased wear resistance over that of the 1.5 μm coating and maintains a friction coefficient of 0.3 up to and over 10,000 revolutions. On the addition of excess carbon in the TiCN coating a decrease in friction coefficient is observed as illustrated in figure 3.10 (b). Similar friction coefficients have been found by other authors[15,16]. The addition of excess carbon during the deposition gives a DLC type amorphous layer. The decrease in friction coefficient is due to a graphitization layer which is created when hydrogen is released from the sp^2 and sp^3 carbon bonds. These hydrogen atoms are introduced into the amorphous layer during the deposition process. During a wearing of the coating using the pin-on-disk tester, the heat caused by the sliding/rubbing action of the pin against the coating releases the hydrogen leaving the graphite layer which has lubricating properties. If there is a higher quantity of carbon in the coating there will be more hydrogen released and a larger graphite layer, which will lead to a decrease in friction coefficient[17]. A lower friction coefficient will also give an increase in wear resistance due to a transfer layer where part of the graphite layer is

transferred to the pin. This gives an extra lubricating effect which increases the wear resistance.

3.4.3 Titanium containing diamond like carbon (Ti-DLC)

Ti-DLC was deposited onto flat stainless steel substrates and analysed by the characterisation techniques outlined in chapter 2.

X-ray diffraction was used in the examination of the crystalline structure of the Ti-DLC coating. No pattern was obtained. This would indicate a lack of crystal structure and a presence of a mostly amorphous coating.

Figure 3.11: A micrograph of a fractured Ti-DLC coating. The dense structure of the coating can be clearly seen. No columns or grain boundaries can be seen.

The micrograph in figure 3.11 illustrates the dense type structure associated with Ti-DLC. There is no indication of the presence of a columnar structure. By Thorntons classification model this coating exhibits a dense fibrous zone T type structure.

Ti-DLC had an average critical load of 17 N. The Rockwell indentation test confirmed this value by giving an average HF value of 3 as illustrated by figure 3.12.

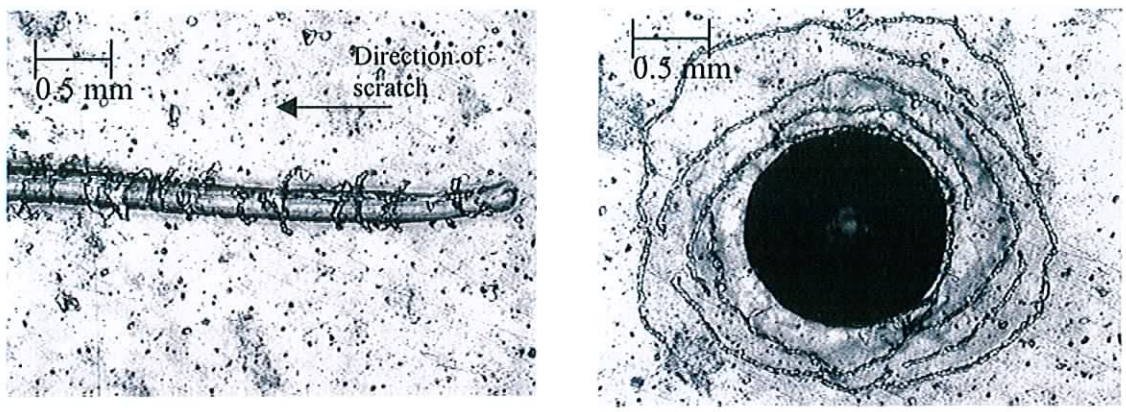

(a) (b)

Figure 3.12: Photographs of (a) a scratch and (b) a Rockwell indentation on a Ti-DLC coating. The cohesive forces can be seen to be poor indicating the high density state of the coating.

The hardness of Ti-DLC was found to exceed a Hk value of 4000. The friction coefficient of Ti-DLC was examined using the pin-on-disk wear tester. The coating was observed to have an average friction coefficient of 0.1. At approximately 180000 revolutions the friction rose abruptly. At this point the pin has worn through to the substrate. Low friction is maintained due to the transfer layer on the pin.

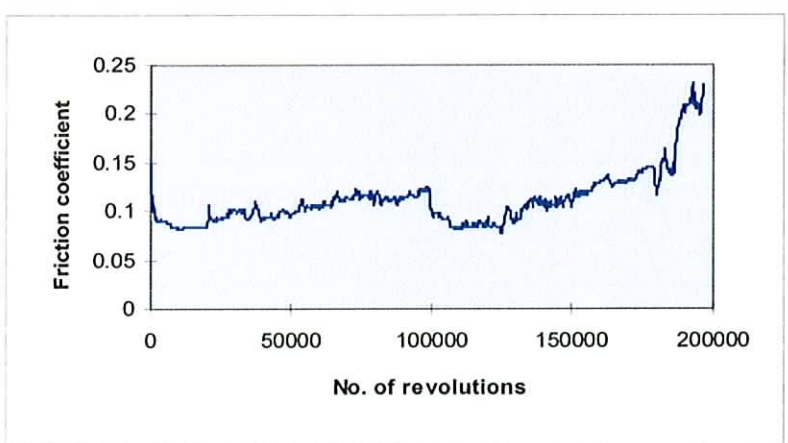

Figure 3.13: Graph of the friction coefficient of Ti-DLC. The friction coefficient has an average value of 0.1, which increases abruptly at approximately 180000 revolutions, due to the pin wearing through to the substrate.

3.4.4 Titanium nitride coated with Molybdenum disulphide (TiN/MoS_2)

As stated in section 1.5.4, this multilayer coating combines the hardness and wear resistance of TiN, with the low friction lubricating effect of MoS_2. The coating is a combination of a thin layer (200 nm) of MoS_2 deposited onto a 3 μm layer of TiN. This coating had similar mechanical properties to that of the TiN coating described in section 3.4.1 as the thickness of the MoS_2 coating did not effect the properties of the TiN coating below it. Therefore the properties of TiN described in section 3.4.1 are the same for TiN/MoS_2. A dramatic change however has occurred to the tribological properties of the TiN coating as illustrated in figure 3.14.

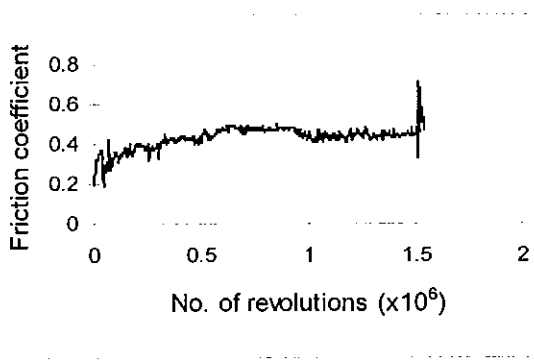

Figure 3.14: Graph of the friction coefficient of a TiN/MoS_2 coating. The coating has an approximate friction coefficient value of 0.4 up to $1.5x10^6$ revolutions.

Figure 3.14 illustrates that the MoS_2 layer lowers the friction coefficient of the TiN coating from its original value of 0.5 to its present value of 0.4. The lower friction is due to the lubricating effect of the MoS_2. A possible explanation for the lower friction value is that in a similar fashion to the Ti-DLC coating, a layer of MoS_2 is transferred to the pin, which, in effect gives an MoS_2 layer sliding against another MoS_2 layer. At $1.5x10^6$ revolutions the pin has worn through to the substrate. This is a significant result and one which has been investigated by other authors[18].

3.5 Conclusion

This section contains a visual summary of the analysis which has been presented in section 3.4. Figure 3.15 illustrates the properties of adhesion, hardness and friction coefficient.

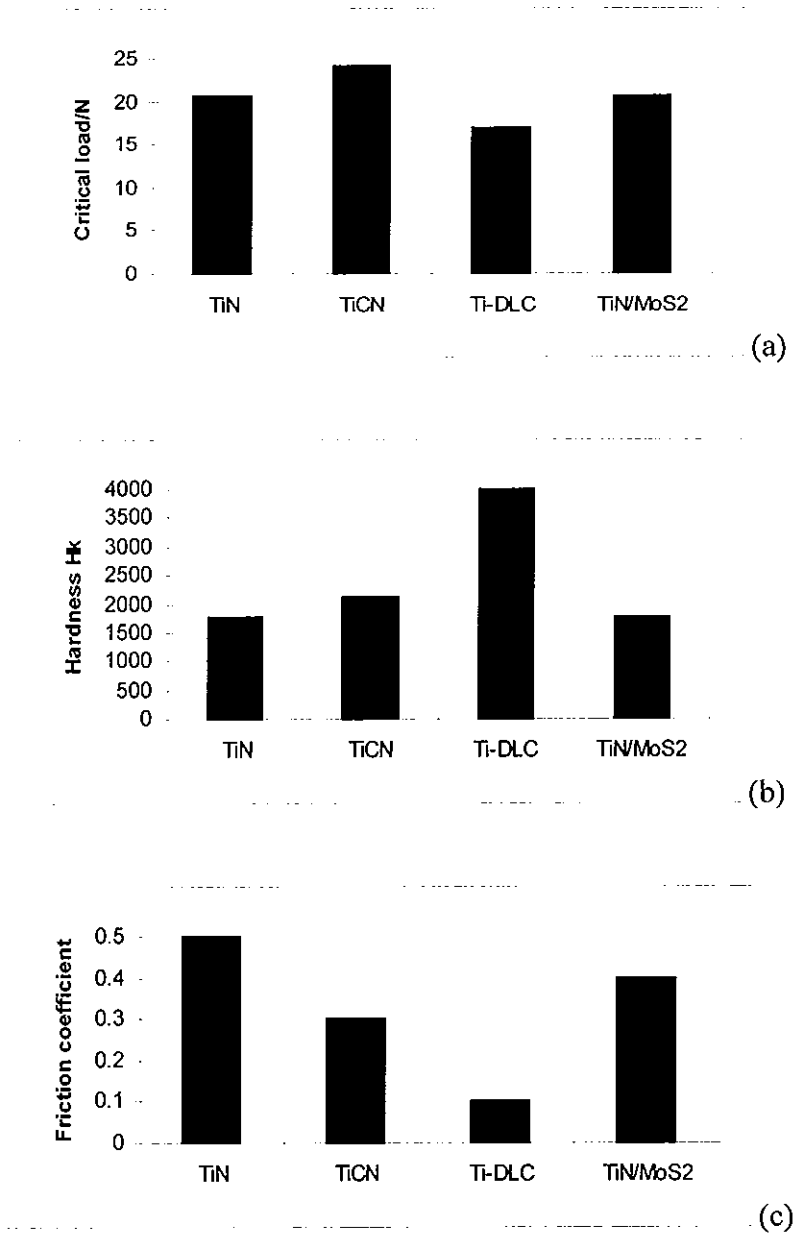

Figure 3.15: A summary of the properties of (a) adhesion, (b) hardness and (c) friction coefficient for TiN, TiCN, Ti-DLC and TiN/MoS_2. The adhesion values are all roughly similar illustrating that all the coatings showed satisfactory coating-substrate adhesion. Ti-DLC showed the highest hardness and also the lowest friction coefficient.

TiN has been used in low speed drilling due to its high hardness and low friction coefficient whilst TiCN has been used in high speed drilling and cutting due its superior hardness and friction coefficient. Ti-DLC is a relatively new coating but should find application in similar industries as TiN and TiCN.

3.6 References

[1] Asymmetric bipolar pulse DC- an enabling technology for reactive PVD, J.C. Sellers, 39th An. Tech. Conf. Proc. (1996).

[2] P.D. Feischauer, M.R. Hilton and R. Bauer, Aerospace report, 1990.

[3] Physical Chemistry, P.W. Atkins, Third edition, 1986, p. 763.

[4] Introduction to Quality Engineering, Genichi Taguchi, Asian Productivity Organisation, 1986.

[5] Morphology of epitaxial TiN (001) grown by magnetron sputtering, Brian Kerr.

[6] Lou et al, Surface and Coatings Technology, 90(1997) 123-127.

[7] L.P. Ward, K.N. Strafford, C. Subramanian and T.P. Willis, Proc. of the Int. Conf. on Advances in materials and Processing Technologies, August 1993.

[8] J. Takadoum et al Surface and Coatings Technology, 88 (1996) 232-238.

[9] A. A. Voevodin, C. Rebholz, J.M. Schneider, P. Stevenson, A. Matthews, Surface and Coatings Technology, 73 (1995) 185-197.

[10] I. Efeoglu, R.D. Arnell and S.F. Tinston and D.G. Teer, Surface and Coatings Technology, 157 (1993) 61-69.

[11] R. Messier, A.D. Giri and R.A. Roy, J. Vac, Sci. Technol, A. 2(2) (1984) 500.

[12] A comparison between the tribological and mechanical properties of TiN and TiCN, N. Donnelly, M. McConnell, D. P. Dowling, J.D.O'Mahony Proc. of the 2nd Int. Sym. on Nitrides, UL, Ireland.

[13] J. Takadoum, H, Houmid Bennani, Surface and Coatings Technology, 96 (1997) 272-282.

[14] J. Deng et al, J. Vac. Sci. Technol. A 1293) May/Jun 1994.

[15] Y.Y. Guu, J. F. Lin, C. Ai, Thin Solid Films 302 (1997) 193-200.

[16] Y.Y. Guu, J.F. Lin, C. Ai, Thin Solid Films 287 (1996) 16-24.

[17] Y. Liu, A. Erdemir, E.I. Meletis, Surface and Coatings Technology, 86-87 (1996) 564-568.

[18] V.C. Fox, D.G. Teer, J. Hampshire, Paper ref. E1-2-9, Int. Conf. on Metallurgical Coatings and Thin Films, April, 1998.

Chapter 4 : Application of coatings to needles

This chapter will deal with the application of the TiN, TiCN and Ti-DLC coatings, which have been deposited on flat stainless steel substrates, onto textile needles. Initially a brief introduction will be given on the textile company and their manufacturing process. The problem with the wear on needles during bandage fabrication will be discussed followed by a discussion of the deposition and testing of the needles. The wear on each of the coated needles will be discussed using profilometry results. The chapter will finish with conclusions and some suggestions for further work.

4.1 Introduction to bandage fabrication

As stated in the introduction to chapter 3 this project had a two tiered approach to it. Initially coatings were deposited onto flat stainless steel substrates to optimise the deposition conditions. Once optimised conditions were achieved, the coatings were deposited onto textile needles.

These needles are used by a company located in Co. Offaly called 'Midland Bandages Ltd'. This company was formed in the 1980's to manufacture a quality range of bandages for the home and export markets. High speed narrow fabric weaving machines are at the centre of the operation. Their products range from sling bandages down to everyday plasters. Different quantities of cotton, viscose and nylon are woven to make the bandages which, depending on the quantity and type of each material used, will have a different application. Each of the thread materials are stored on large spools. The thread is fed into a central weaving machine as illustrated in figure 4.1.

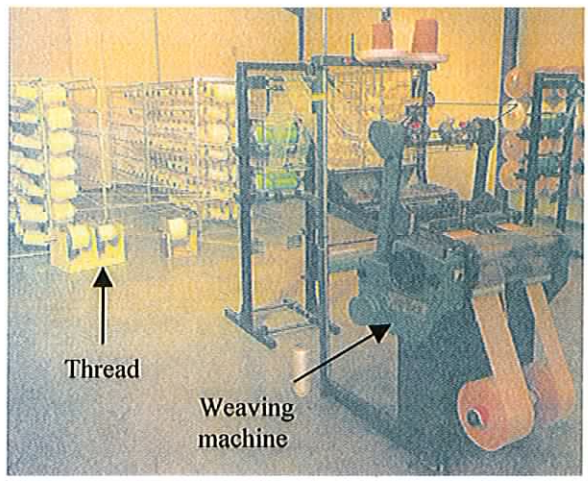

Figure 4.1: The weaving process at midland bandages. The thread leaves the spools and travels to the weaving machine where it manufactures bandages.

The thread is fed through a series of rollers to keep its tension high. Tension springs are also used to facilitate the tension and to act as a guide for the thread. The final stage of the weaving process uses a needle working at 1050 R.P.M. to weave the fabric. As the thread is in a state of high tension and is pulled through the tension springs and the needles at high speed, a certain quantity of wear occurs at these two stages as illustrated in figure 4.2.

(a)

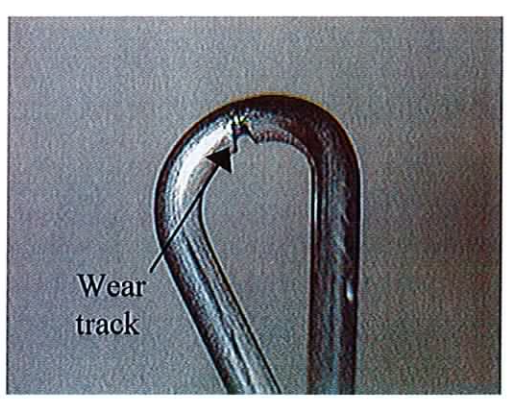

(b)

Figure 4.2: Photographs of (a) wear on a textile needle and (b) wear on a tension spring. The thread is pulled through both the needle and the tension spring continuously to form the groove.

This extent of wear on the textile tools causes the thread to snap after a certain time. The cost of needle and tension spring replacement can be large, but also the cost to the manufacturer due to "downtime" of the process can be substantial. By coating these tools with wear resistant coatings, it should have been possible to extend their lifetime. In doing so the time interval between tool replacement should increase, leading to a decrease in "downtime" of machinery. Hence, an increase in productivity.

Due to the cost involved with using the needles and tension springs (i.e. the needle is £70 to buy), less expensive needles, as highlighted in figure 4.3, were used for test purposes.

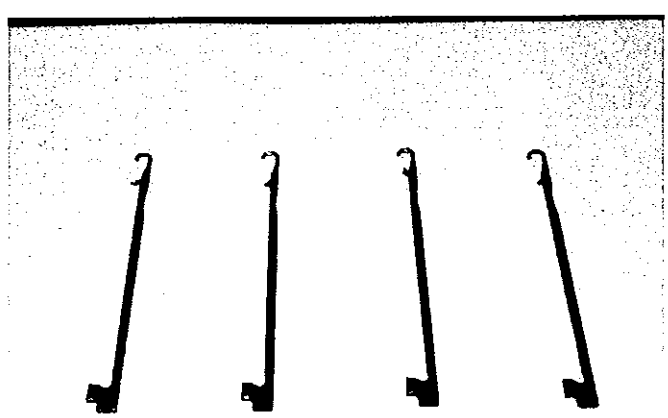

Figure 4.3: Photograph of the test needles used in the project. They are pictured from left to right, uncoated, TiN, TiCN and Ti-DLC respectively.

An optical metalographic examination showed that the test needles were made from a high carbon steel containing up to 0.8% carbon. It has a martensitic structure with fine carbides. Needles were coated with TiN, TiCN and Ti-DLC.

As the needles were of a different geometry to that of the flat samples, the characterisation techniques used on the flat substrates could not be used. Therefore, the coatings could not be quantitatively or qualitatively compared. It was necessary to design and construct a rig to

simulate the wear process that the needles and tension springs undergo while in the industrial weaving process. The following section will discuss the wear tester in detail.

4.2 Wear tester for needles

4.2.1 Introduction

A test rig was constructed to simulate the action of a needle in a high wear environment. The needles used in the industrial process needed to be replaced after approximately five to six months. The tension springs were replaced after approximately a month. This wear was due to the constant action of the thread on the eye of the needle and on the tension springs. The test rig that was built would ideally simulate the action of the thread on the needles and tension springs but as time was an issue it had to be made in such a way that the coated needles showed signs of wear after as short a time as possible.

The rig went through a number of stages of designs and constructions, the more important stages of which are outlined in sections 4.2.2 to 4.2.4.

4.3 Rig 1

The initial rig, seen in figure 4.4, consisted of a motor pulling thread onto an empty spool, through the eye of the needle, which was fed off a 5000 m spool of Corespun polyester thread. The empty spool was made from a nylon material and was rotated by a medium duty motor (Radionics model no.-255-9611). The spool of thread was placed on a spindle and a rubber break was attached to it to maintain tension on the thread. As the motor rotated, thread from the spool fed onto the empty spool while wearing at the needle. The needle was clamped in place using an aluminium clamp.

4.3.1 Problems encountered

This design presented a number of problems. Firstly, the needle showed no signs of wear after 5000 m. As the supply of thread was limited, it was decided that the same thread would have to be used a number of times, before being replaced. Therefore, once the empty spool had been filled, the spools could be reversed. However, the thread that was spun onto the empty spool did not do so in an ordered fashion and became entangled on the spool. It could therefore not be used again. Secondly, the tension of the thread could not be maintained at a high enough level to cause wear. When the tension was increased by applying the rubber brake, the thread would snap after a short time. These factors forced this design to be upgraded.

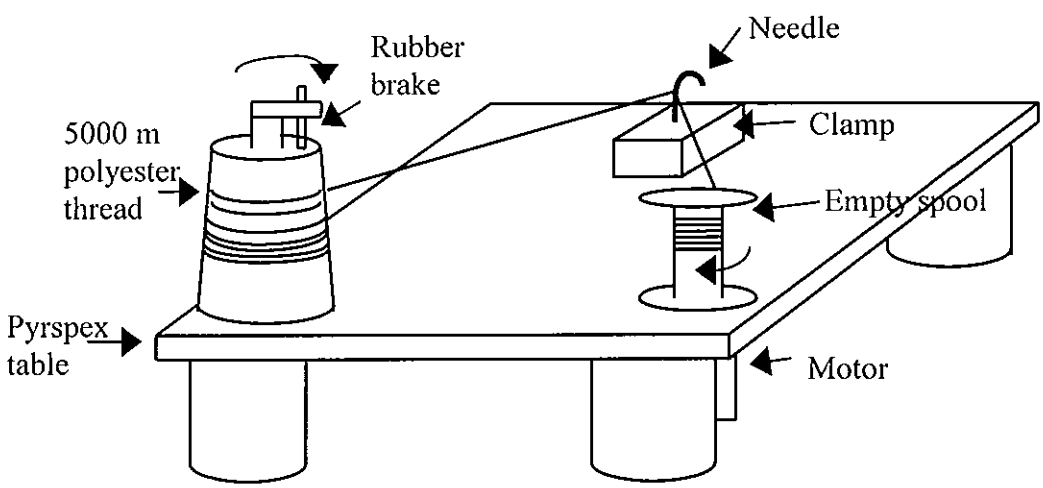

Figure 4.4: Schematic diagram of rig 1. The thread came off the spool onto the motorised spool via the needle, wearing a groove into the needle.

4.3.2 Modifications

Based on the results obtained from rig 1 it was known that stronger thread and a requirement for reproducible tensions on the thread was needed. Therefore fishing line was employed to counteract the snapping of the thread due to its increased strength over the polyester thread. This meant that more tension could be put on the thread which was thought would increase the wear rate. However the fishing line, made from a polymer, had a

low coefficient of friction and did not wear the needle. Therefore the original thread had to be used.

4.4 Rig 2

The second design was based on the requirement to reduce the quantity of thread used in the wearing process. To do this, the needle was rotated while the thread was held in a fixed position relative to the needle. The thread became worn quickly and snapped when in a stationary position. To rectify this problem the feeder spool had to feed the thread at a constant slow rate. In order for this to happen, a stepper motor was employed to control this feed rate. The stepper motor setup consisted of the stepper motor (radionics model no. 440-442), a control box (radionics model no.217-3611) and a pulse generator (GW model no. GFG-2D). The frequency of the pulse determined the number of steps in a full rotation of the motor. The needle was clamped onto a rotating spool and the feeder spool was attached to the stepper motor. The thread came off the feeder spool onto the needle, through a ceramic holder held in place by a retort stand and clamp. For comparison purposes the thread was held in place at the same point on each of the needles tested by means of a clamp attached to the rotating spool. The thread was also attached to a load as illustrated in figure 4.5.

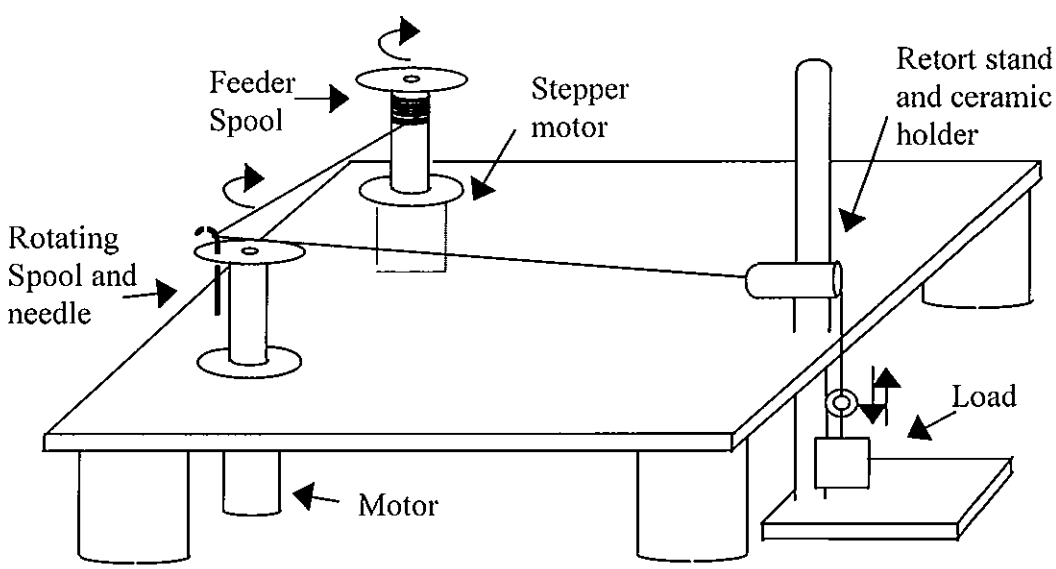

Figure 4.5: Schematic diagram of rig 2. The thread came off the feeder spool. It was then fed onto the needle. The needle rotated while the thread, which was attached to a load, wore a groove into the needle.

The tension on the thread was supplied by a 2.5 N load as indicated by table 4.5, so as to maximise the wear rate. As the needle rotated the thread wore into it causing a wear track which could then be examined.

4.4.1 Influence of load

The maximum amount of wear was necessary on the needle to decrease the length of time the needle needed to be on the wear tester. Different loads were used on the wear tester. These are tabulated in table 4.1. As can be seen in the table, the highest load that could be used on the wear tester, without snapping the thread, was 2.45 N.

Load applied/N	Condition of thread
2.45	Did not snap
2.9	snapped
3.4	snapped
3.9	snapped

Table 4.1: Loads used on the wear tester. Each of the loads in the table were tested on the wear tester to establish the highest load that could be used.

4.4.2 Influence of thread thickness

Varying thickness' of thread were tested to investigate their effect on the wear of the needle. The thread types were 75, 100, 120, 180. Each of the numbers listed corresponds to a different thickness in thread. The 75 type thread is the thickest of the four types. Very high tension was required to speed up the wear process. The thinner thread could not support the weight of the load and therefore the 75 type thread had to be used as illustrated in table 4.2.

Thread thickness	Condition of thread under 2.45 N load
75	did not snap
100	snapped
120	snapped
180	snapped

Table 4.2: The four types of thread shown in the table were experimented with to find which would support a 250 g weight (2.45 N Load).

4.4.3 Problems encountered

The problems associated with this wear tester were firstly, that a typical run would take 7-8 days to complete. During this time the thread would sometimes snap randomly. As the thread lengthened and the distance between the ceramic holder and the load increased, the load began to swing. In swinging, the tension on the thread would become unstable. This instability led to the snapping of the thread. The longest period of time that the wear tester was left on for was overnight when the wear process would last for 16 hrs. In this case the load had a distance of 190 cm between the ceramic holder and the ground giving a feed rate of 0.198 cm/min or 11.88 cm/hr. In one hour a length of thread 11.88 cm long wore continuously at the needle head. However, there was also counter wearing of the thread by the needle leading to a decrease in the thickness of the thread. This decrease in thickness effected the strength of the thread so the load on the thread became too great for the thread to hold and therefore caused it to snap. These problems required the design of a new tester to eliminate the wear of the thread and to speed up the entire wear process. This tester was called rig 3.

4.5 Rig 3

Due to the problems, on rig 2, of the thread continuously snapping and the lethargic speed of the experiment, modifications were made to the tester to eliminate them. As illustrated in figure 4.6, a clamp was attached to the retort stand and the thread was passed under an M6 bolt with threads (attached to the load with red insulated wire) and fastened to the bottom half of the feeder spool. Therefore, as the thread was fed off the feeder spool it fed onto it again so that the load stayed in the same position and could be left on indefinitely. Also, the load did not swing and because it was being supported on two sides, an increased load could be used. Loads of 9.81 N, 8.83 N, 7.85 N and 6.87 N were used, of which, only the 6.87 N weight did not snap the thread. This gave a working load of ~ 3.4 N.

This new and final design could be run continuously. A similar quantity of wear to that of rig 2 after 7-8 days was inflicted on the needle after 24 hrs on rig 3. Needles with different coatings could be left on the tester over this period and the wear tracks could be examined and compared.

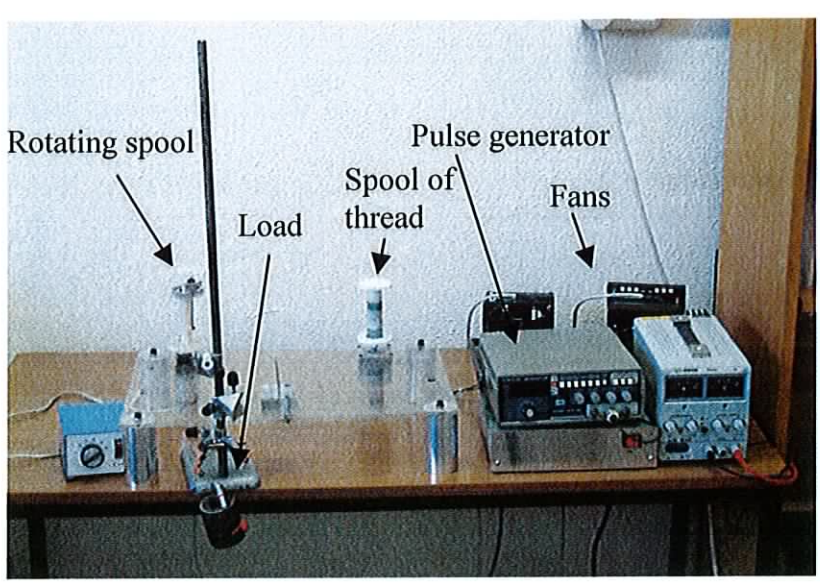

Figure 4.6: Photograph of the final construction (rig 3) of the wear tester. The thread, which was attached to a load, came off the spool, wore at the needle and returned to the spool so as the tester could be left on indefinitely.

4.6 Coated needle deposition

The needles used in the project are shown in figure 4.3. As the needle was rotated on the wear tester the entire circumference of the needle was worn by the thread. It was important that all faces of the circumference of the needle were coated. If a coating was deposited onto only one face of the needle then, during testing, a 'knife edge' effect would occur. This 'knife edge', as illustrated in figure 4.7, occurs due to a hard material (the coating) being next to a soft material (the needle substrate). The soft material has an increased wear rate over that of the hard material. This difference in rates caused a sharp 'cliff' to be formed between the two. This 'knife edge' acts as a blade cutting the thread as it passes over it. Due to this phenomenon, it was necessary that all faces of the needle were coated.

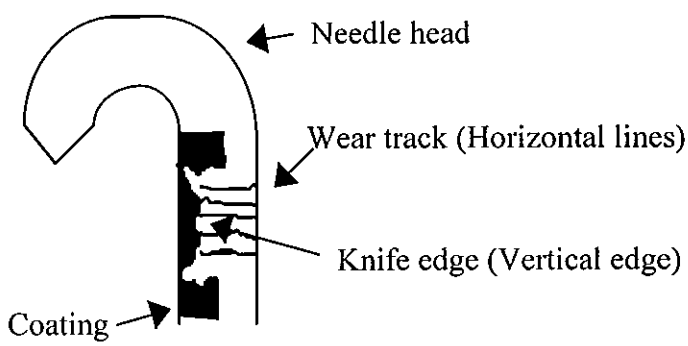

Figure 4.7: Schematic diagram of a coated needle with a 'knife edge' problem. The coating has been deposited onto the front face of the needle. The difference in wear resistance between the hard and soft material caused the 'knife edge' effect.

4.6.1 Rotation of the substrate

To deposit a coating on all faces of the needle it was necessary to rotate the substrate holder while deposition took place. This was possible due to the incorporation of the biased substrate holder with a DC motor and drive belt. The deposition parameters used were the same as those outlined in section 3.2.3, only the substrate was rotated.

However, there were problems associated with rotation of the needle. While rotating the needle the sides of the substrate holder (which was made of metal) came close to the

magnetron which caused interference in the deposition due to plasma instabilities, as illustrated in figure 4.8. The coatings deposited when rotating the needle had poor adhesion and in all cases, delaminated. To counteract this problem the quantity of metal on the substrate holder was reduced. This caused changes in the power level of the biasing supply and the interference with the deposition remained. As no high quality films were deposited by constant rotation of the needle, experiments on stepped rotation of the needle at intervals of 90° were carried out. This would ensure that minimum inference was inflicted on the plasma and it should remain stable. Also, the thickness of the coating should have been uniform. At each 90° interval the coating was deposited onto the needle for 5-10 mins.

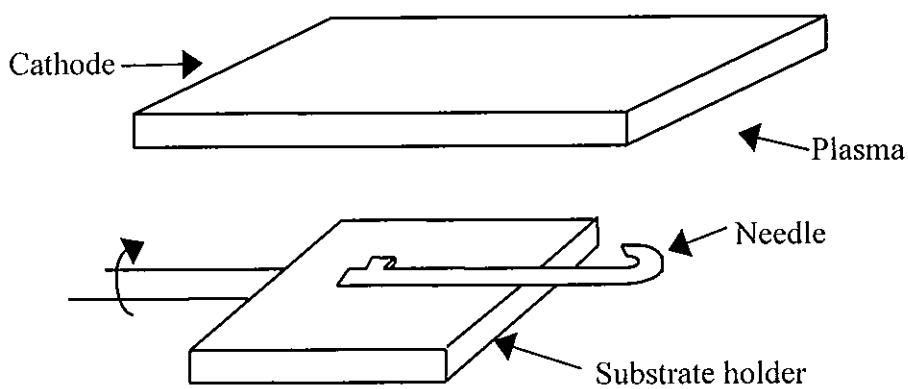

Figure 4.8: Rotating substrate holder and needle beneath the cathode. The rotation of the needle caused instabilities in the plasma and therefore the deposition process also.

Due to the soft nature of the MoS_2 material, during early experiments on the TiN/MoS_2 needle the MoS_2 would flake off the needle easily leaving only TiN underneath. It therefore proved not fitting for this type of application. Coatings of TiN, TiCN and Ti-DLC were deposited onto the needles and then tested.

4.7 Needle testing

For comparison purposes there will be two sets of results in this section. There is four needles in each set, an uncoated needle, TiN, TiCN and Ti-DLC coated needles. The first set will come from the needles that were tested on rig 2 and the second will come from needles that were tested on rig 3. The needles were analysed using a profilometer. The profilometry work was carried out at N.C.L.A, N.U.I. Galway using a Zygo Newview199

scanning white-light interferometer. As the wear around the needle was uniform the analysis was performed on one side of the needles. The area of analysis is illustrated in figure 4.9 and in more detail in figures 4.10 and 4.13.

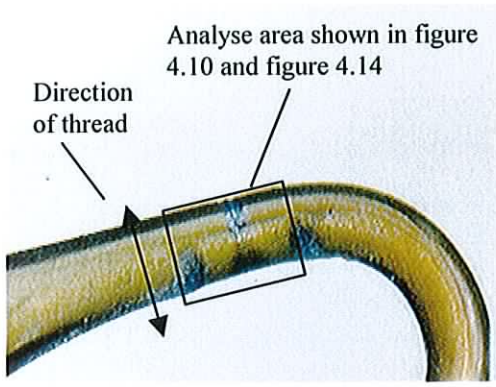

Figure 4.9: Photograph of the head of a TiN coated needle showing the analyse area which is magnified in figure 4.10 and 4.14.

The silver coloured area in the centre of the rectangle in figure 4.9 is the area of wear on the needle head caused by the wearing action of the thread during a run on the wear tester. In this particular example the TiN coating has delaminated (the silver coloured area) at the back of the needle due to non-rotation of the needle during deposition. The double-ended arrow indicates the direction that the thread wore the coating, hence the obvious 'track' in the centre of the rectangle.

Wear results from rig 2 and rig 3 will be used so as to compare the differences between the two techniques of wear and are shown in sections 4.7.1 and 4.7.2.

4.7.1 Wear results of rig 2

The results in this section were obtained using rig 2 (shown in section 4.4) to wear the needles. In this case the uncoated needle was worn until the thread snapped. This occurred at approximately 18 m and took 7-8 days. The coated needles were tested for the same length of thread (18 m). Analysis was carried out using a profilometer. Photographs of the wear tracks made on the needles by rig 2 are shown in figure 4.10. They are magnified photographs of the area shown in figure 4.9.

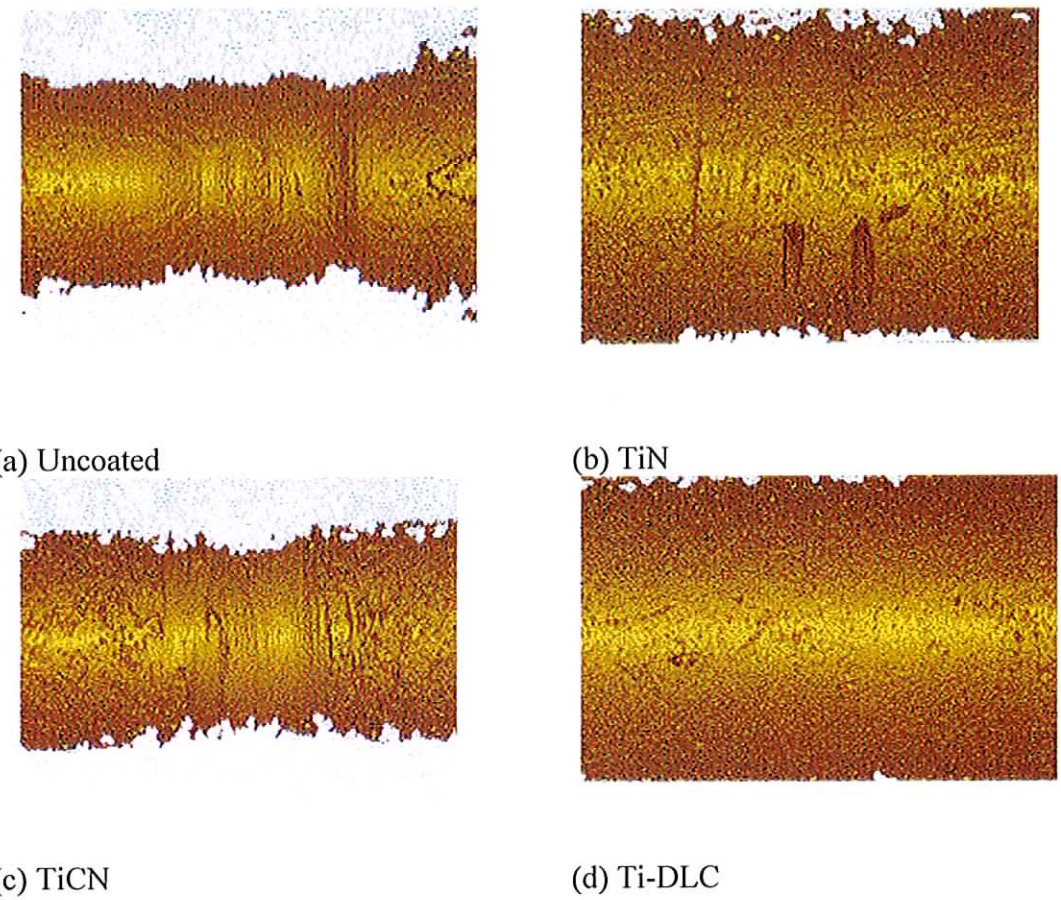

(a) Uncoated (b) TiN

(c) TiCN (d) Ti-DLC

Figure 4.10: Photographs (taken using a profilometer) of wear tracks made on coated and uncoated needles using rig 2. The needle is held horizontally and the wear track can be seen clearly running vertically in (a), (b), (c) and (d).

The photographs in figure 4.10 show that the largest quantity of wear appears to have occurred on the uncoated and TiCN. The Ti-DLC had the highest wear resistance of the coatings tested. A groove has formed on the uncoated needle as illustrated in figure 4.10(a). This groove has many asperities, most of which are sharp. It is these asperities that most probably led to the snapping of the thread during the wearing of the needle. The TiN coated needle appears to have a wear track and two small grooves on the surface. The thread in this case has not worn through to the substrate which would indicate that TiN has excellent wear resistance in this type of application. The grooves in the surface, however, would indicate that the thread was beginning to wear into the coating. If the needle had been left

on the wear tester over a longer period of time the grooves would have grown in diameter and depth. The TiCN coating appears to have been worn quite extensively by the thread, but in the case of the Ti-DLC, only a slight polishing has taken place. This behaviour would not be one that was expected given the excellent friction coefficient and hardness exhibited by TiCN when deposited onto flat substrates. A possible explanation for this phenomenon is that, as the adhesion of the coatings on the needles could not be quantitatively or qualitatively measured, in some areas of the TiCN coating, the adhesion was poor. The poor adhesion in a small area could 'spall' (explained in figure 2.3) off. If some of the coating has delaminated, erosion of the rest of the coating from the point of delamination could have occured quite easily. A 2-D contour line profile on each of the wear tracks was taken using the profilometer. The width of each of the wear tracks were plotted onto one graph as shown in figure 4.11. The depth profile of the wear track on each of the needles can be visually compared.

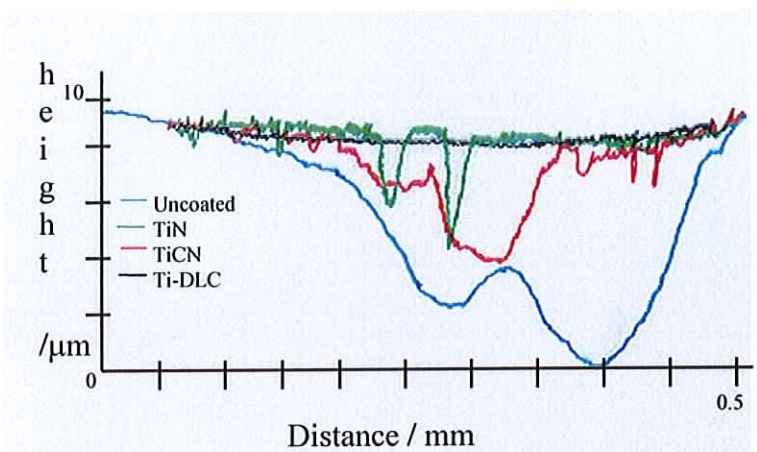

Figure 4.11: Profilometry results for coated and uncoated needles having been worn using rig 2. It can be seen that Ti-DLC exhibits the highest wear resistance in comparison to the uncoated needle and the other coated needles.

Figure 4.11 illustrates that the thread has worn 10 µm into the uncoated needle at one point. The plot illustrates that the coated needles exhibit significantly less wear than that of the coated needle. The Ti-DLC has the highest wear resistance. This is also illustrated in figure 4.10. The worn area was measured for each of the wear tracks in figure 4.11 and the results obtained are given in table 4.3.

Sample	Area/nm^2
Uncoated	2.45
TiN	0.35
TiCN	1.14
Ti-DLC	0.20

Table 4.3: The area above the curve of a 2-d contour wear track for the uncoated and coated needles. The Ti-DLC coated needle exhibits the least wear.

In figure 4.12 a 3-D plot of the each of the wear tracks is given which again demonstrates the higher wear resistance of Ti-DLC as compared to the other coated and uncoated needles.

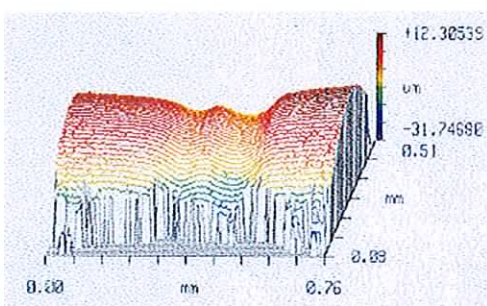

(a) Uncoated

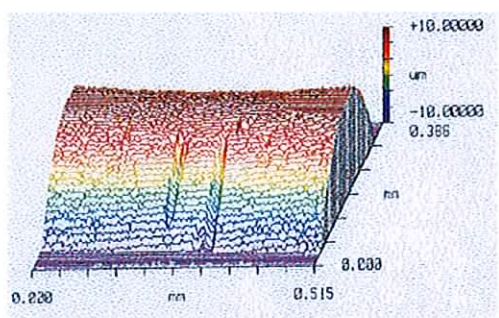

(b) TiN

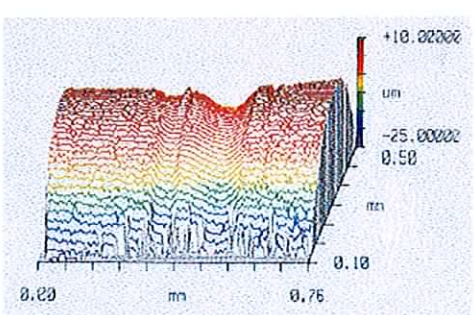

(d) TiCN

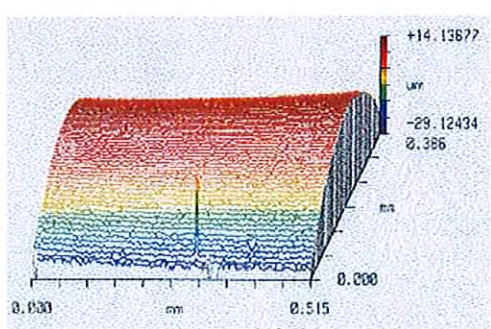

(e) Ti-DLC

Figure 4.12: 3-dimensional plots of the wear on the coated and uncoated needles. The wear can be clearly seen in all cases.

In conclusion the order of increasing wear resistance is:

$$uncoated < TiCN < TiN < Ti\text{-}DLC$$

This result would appear to be surprising given that on increasing the level of carbon in the coating the friction coefficient should decrease and it would be expected that TiCN would have a higher wear resistance than TiN. This conclusion is supported by the very low wear observed for the Ti-DLC. A possible explanation for this result was obtained when the opposite sides of the needle heads for table 4.3 were examined. It was found, based on visual examination, that the wear tracks for the uncoated, TiN and Ti-DLC needles were broadly similar around the circumference of the needle head. The wear on the TiCN coated needle in contrast was found to be very inhomogeneous with very little wear observed for the side not measured in table 4.3. This is illustrated in figure 4.13. It would therefore lead us to believe that the area chosen to be analysed on the TiCN coating had poor adhesion possibly due to a contaminant in the chamber or on the sample. Due to the excellent wear resistances exhibited in figure 4.13 it was therefore concluded that the order of wear resistance was as follows:

$$uncoated<TiN<TiCN<Ti\text{-}DLC$$

As demonstrated by the difficulties associated with the inhomogeneous wear exhibited for the TiCN coated needle, a major source of error for these wear measurements is the inability to obtain quantitative data over the entire area of the worn surface. The results can therefore only be considered as semi-quantitative. A second problem with the test method was having to frequently replace the thread (~15 times per run) during the 7-8 days it took to obtain the measurements on each needle. This long period of time over which the test was run meant that factors such as the temperature on the wear track was not consistent at all times. This would influence the wear on the needles. In order to overcome this latter source of error a new wear tester was designed (rig 3), in which the thread did not have to be replaced during the needle wear test.

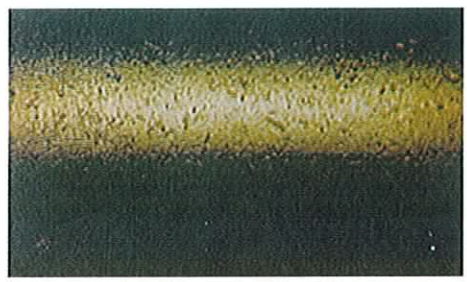

Figure 4.13: Photograph of the opposite side to that of the analysis area shown in figure 4.9 for the TiCN coating. The TiCN exhibits a slight polishing of the surface of the coating.

4.7.2 Wear results from rig 3

This section describes the wear on needles which were worn using rig 3 (described in section 4.5). The needle, when tested on rig 3, was clamped in the rotating spool. The thread was tied via the needle through the ceramic holder and back to the rotating spool as shown in figure 4.6. The rotating motor and stepper motor were switched on and were run for 24 hrs. The analysis area of the needles is shown in figure 4.9. The wear tracks made by rig 3 were analysed using a profilometer. The photographs of one area of the needles is shown in figure 4.14. The fact that the samples in this section could be run continuously for 24 hrs meant that there were less sources of error than that of rig 2 and therefore this set of results should reflect a more accurate representation of the wear inflicted on an industrial needle.

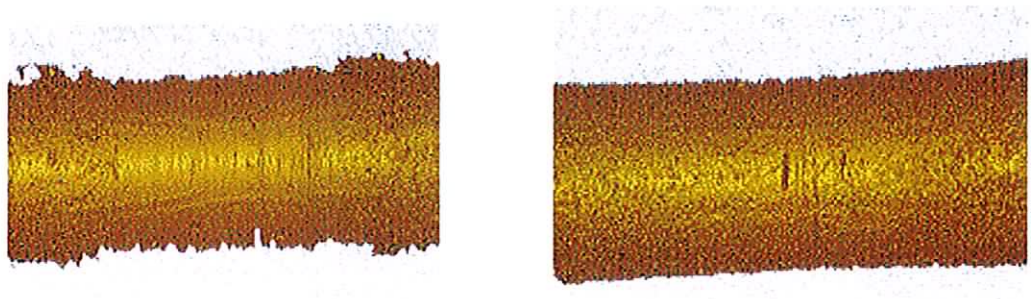

(a) Uncoated (b) TiN

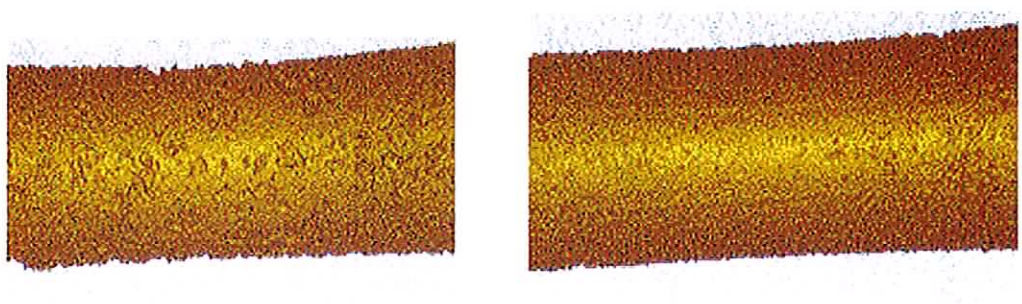

(c) TiCN (d) Ti-DLC

Figure 4.14: Photographs of wear on coated and uncoated needles. The difference in the quantity of wear between the uncoated and coated needles is apparent. There is notable pitting in the TiCN coating.

A notable feature of figure 4.14 is that each of the wear tracks are very similar to those shown in figure 4.10 for rig 2. As illustrated in figure 4.14(a) there is extensive wear on the uncoated needle. The thread has formed a groove in the needle, which is the result expected after a time period of 24 hrs. On the needle coated with TiN the thread has worn through the coating at discrete points forming small grooves. The TiCN coating on the needle appears to have resisted wear quite well. Although slight 'pitting' can be seen. This 'pitting' is not a common feature of TiCN but can be the result of a coating with poor adhesion or inhomogeneous deposition. On the Ti-DLC coated needle only a slight polishing is apparent on the surface of the coating which would be expected from a coating with such a low friction coefficient. Figure 4.15 shows a line profile of the wear tracks.

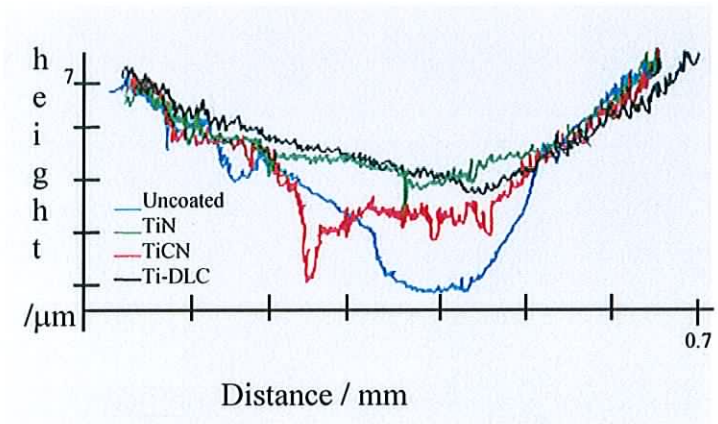

Figure 4.15: Cross section of the wear tracks on coated and uncoated needles using a Zygo Newview 100 scanning white-light interferometer. The Ti-DLC and the TiN appear to have similar quantities of wear.

The plot in figure 4.15 shows that both TiN and Ti-DLC have a high wear resistance in comparison to the TiCN and the uncoated needle. This trend is also represented by the area above the curve of the wear tracks tabulated in table 4.4.

Sample	Area/nm^2
Uncoated	1.48
TiN	1.01
TiCN	1.38
Ti-DLC	1.04

Table 4.4: The area of a 2-d contour wear track for the uncoated and coated needles. In this case the TiN coated needle is found to have the highest wear resistance. Although the difference in wear between the TiN and Ti-DLC coating is almost negligible.

The area values also illustrate that TiN and Ti-DLC are very similar in wear resistance. Figure 4.16 shows oblique plots of the needles. There does not appear to be a large difference in wear between each of the needles on shown in figure 4.16. We must therefore rely on the information given in figure 4.14 and 4.15.

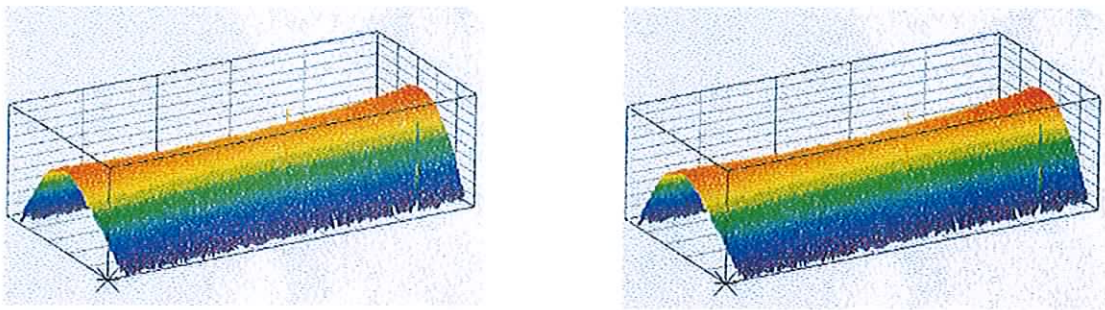

(a) Uncoated (b) TiN

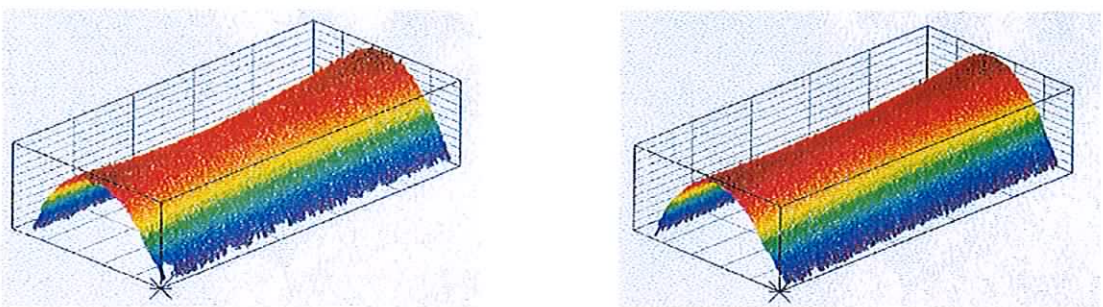

(c) TiCN (d) TiDLC

Figure 4.16: Oblique plots of coated and uncoated needles worn by rig 3. The wear track can be seen in each of the plots.

It can be concluded that the order of increasing wear resistance is given as:

uncoated<TiCN<TiN=Ti-DLC

Similar to that in section 4.7.2 this result forced the coated needles to be turned 180° to that shown in figure 4.9 and inspected for wear. The wear on the coatings on this face of the needles appeared to be similar to that of the original measured side, apart from the TiN coating which is illustrated in figure 4.17. On this area of the TiN coating, a large wear track is visible and the thread had worn through to the substrate.

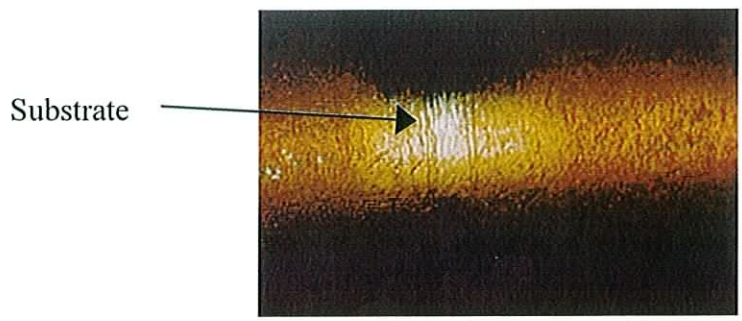

Figure 4.17: A photograph of a TiN coating on a needle after the needle had been turned 180° to that shown in figure 4.9. Due to the action of the thread the coating has been worn through to the substrate.

Similar to that of the TiCN coating worn by rig 2, the photograph in figure 4.17 demonstrates that the wear resistance of the TiN coating was significantly less than that illustrated in figure 4.14(b), figure 4.15 and table 4.4. As the TiCN coating had homogenous wear on both sides of the needle and at no point did it wear as badly as to show the substrate, it can be said that TiCN had a higher wear resistance to that of the TiN coating. Therefore the order of increasing wear can be summarised as:

uncoated<TiN<TiCN<Ti-DLC

All results shown conclude that Ti-DLC has superior wear resistance performance in this type of application in comparison to the other uncoated and coated needles. It must be concluded, therefore, that Ti-DLC would be the ideal coating to choose if maximum enhancement of the wear life of textile needles is to be achieved.

There is no conclusive evidence to suggest why there was a large amount of pitting in the TiCN coating. Usually, pitting on a coating can mean that the surface of the coating was contaminated and that there was no adhesion between the coating and substrate in the contaminated area. This contamination could have been caused in the chamber itself or may have been present on the substrate before being placed in the chamber. As the sample preparation of the substrate in all cases was quite thorough, it is more likely that the contamination came from inside the chamber.

Chapter 5: Conclusion

5.1 Conclusions

The enhancement of the wear life of needles used in the textile industry has been studied. Coatings of TiN, TiCN, Ti-DLC and TiN/MoS_2 were deposited onto flat stainless steel substrates to optimise the parameters used in the deposition of the films. A Taguchi experimental design programme was used to lower the number of experiments required.

Once optimised conditions had been established, coatings of TiN, TiCN and Ti-DLC were deposited onto textile needles. These needles were tested using a wear tester. The wear tester went through a number of designs and constructions before the final tester was complete. Once completed the coated and uncoated needles were worn for certain periods of time and then analysed for wear tracks using optical microscopy and profilometry. All needles showed signs of wear. The uncoated needles showed the most significant quantity of wear. The Ti-DLC coating showed the highest wear resistance except in one case where the TiN coated needle appeared to have a similar wear resistance to that of the Ti-DLC. As the excellent wear resistance of the TiN coated was not consistent the Ti-DLC proved to have the most desirable wear properties in this type of wear application.

5.2 Suggestions for further work

In this work deposition of the coating onto the needle was limited by their uniformity. Rotating of the needle to achieve uniform coating proved difficult as the plasma became unstable. More work could be done to investigate the instability of the plasma during the rotation process. By varying the size of the substrate in the chamber the power levels increase and decrease accordingly. Investigation of a direct correlation between the size of the substrate and the power level could be performed.

An investigation into the performance of the needle in a textile industry could be performed to establish whether the coated needle demonstrated the same type of wear resistance in a real life situation.

5.3 Published work

"A comparison between the mechanical and tribological properties of TiN and TiCN", N. Donnelly, M. McConnell, D.P. Dowling and J.D. O'Mahony, Proceedings of 2nd international symposium on nitrides, University of Limerick, 9th June 1998.

"The effect of thermal treatment on the tribological properties of PVD coatings", M. McConnell, D.P. Dowling, N. Donnelly, K. Donnelly, M. McGuinness, Proceedings of plasma surface Engineering 1998, Garmisch-Partenkirchen, Germany.

Glossary of terms

1. Point defect

This is a defect in the lattice of a crystal. It can be a vacancy in the lattice (Schottky defect), a vacancy self-interstitial (Frenkel defect), an interstitial atom or a substitutional atom.

2. Target Poisoning

This is the build up of an insulating film on the target surface. This occurs during reactive sputtering when the sputtered material reacts with the reactive gas in the chamber and a new compound is formed which normally is deposited onto the substrate but can also condense onto the target creating an insulating film. A capacitor can be formed between the plasma being a conductor and the target being another conductor. DC current cannot flow through the dielectric made and therefore no sputtering can occur as no argon ions are attracted to this area.. Hence the target has been poisoned. This poisining can also lead to arcing which often dissrupts the deposition of stoichiometric thin films.

3. O-ring

A circular piece of rubber used to seal gaps between two connecting pieces. Usually used for short term connection, but can be used for more sustained lengths of time.

4. Equiaxed grains

These are grains in a microstructure where the axes all follow the same direction i.e. they may all be (100) or all (010).

5. *Plastic deformation*

The theory of elasticity states that if a material is strained past its elastic limit then plastic deformation begins.

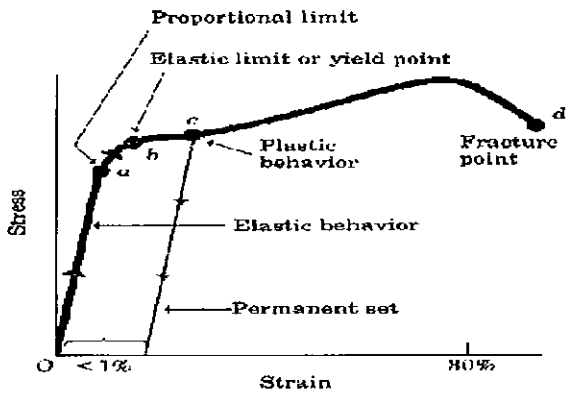

Figure 1: The stress - strain curve of a ductile metal under tension. The graph demonstrates elastic behavior (0-a), plastic behavior (b-d) and the fracture point of a material (d).

The curve in figure 1 shows the pattern a ductile mateal would take under tension. From 0 to a it demonstrates purely elastic behavior corresponding to Hookes law. Therefore the material will return to its original position after the strain. From a to b stress and strain are not proportional but again the material will return to it original position. At point c plastic deformation begins and at point d it ends with frature of the material. If the material is brittle the fracture will occur shortly after point c.

6. Tribology

Tribology has been described as the science and technology of interacting surfaces in relative motion and of related subjects and practices [Engineering tribology, J. A. Williams]. Tribology deals with friction, lubrication and wear. The tribilogical properties of a material would therefore describe its frictional and wear resistance properties.

7. Interphase

An interface is the point where two materials are joined. An interphase is the area where two materials are linked by another material which has properties common to both materials as illustrated in figure 2.

(a) (b)

Figure 2: Schematic diagram of (a) the interface between two materials and (b) the interphase between two materials.